

1 **A longitudinal study of endocrinology and foraging ecology of gray whales prior**
2 **to death based on baleen analysis.**

3 **Author list:**

4 Alejandro Fernández Ajó^a *
5 Clarissa Teixeira^b
6 Daniela M. D. de Mello^c
7 Danielle Dillon^{d†}
8 James M. Rice^e
9 C. Loren Buck^d
10 Kathleen E. Hunt^f
11 Matthew C. Rogers^g
12 Leigh G. Torres^a

13 ^a Geospatial Ecology of Marine Megafauna Lab, Marine Mammal Institute, Department of Fisheries,
14 Wildlife and Conservation Sciences, Oregon State University, Newport 97365, OR, USA.

15 ^b Marine Mammal Institute, Department of Fisheries, Wildlife and Conservation Sciences, Oregon State
16 University, Newport 97365, OR, USA.

17 ^c Department of Physiology, Institute of Bioscience, University of São Paulo, São Paulo, 05508090, SP,
18 Brazil.

19 ^d Department of Biological Sciences, Northern Arizona University, Flagstaff, AZ 86011, USA.

20 ^e Oregon Marine Mammal Stranding Network, Marine Mammal Institute, Oregon State University,
21 Newport 97365, OR, USA.

22 ^f George Mason University & Smithsonian-Mason School of Conservation, 1500 Remount Rd, Front
23 Royal, VA 22630, USA.

24 ^g NOAA, National Marine Fisheries Service, Alaska Fisheries Science Center Auke Bay Laboratories,
25 Juneau, AK 99801, USA.

26 †Present address: New England Aquarium, 1 Central Wharf, Boston, MA 02110

27 ***Corresponding author:**

28 Email address: fernaaale@oregonstate.edu (A. Fernández Ajó)

29 Declarations of interest: none

30 **CRedit author statement:**

31 **A. Fernandez Ajó:** Conceptualization, Methodology, Investigation, Formal analysis, Writing - original
32 draft, Writing - review & editing. **C. Teixeira:** Conceptualization, Methodology, Investigation, Formal
33 analysis, Writing - original draft, Writing - review & editing. **J. Rice:** Samples acquisition, Review &
34 editing. **D. Mello; D. Dillon:** Conceptualization, Methodology, Lab-work; **M.C. Rogers:** Methodology,
35 Investigation, Formal analysis, Review & editing. **C.L. Buck; K.E. Hunt, and Leigh Torres:**
36 Conceptualization, Methodology, Resources, Writing - review & editing, Supervision, Funding
37 acquisition.

38 **HIGHLIGHTS**

- 39 • Baleen analysis of hormones and stable isotopes is a powerful tool to enable a comprehensive
40 and retrospective assessment of stress, reproduction, and nutritional status of the gray whale.
- 41 • Gray whale baleen holds an endocrine and isotopic record of the last 1.3 years of the individual
42 prior to death.
- 43 • Quantification of baleen glucocorticoid content enables discrimination between chronic illness
44 and acute stress as cause of death.
- 45 • Fluctuations in baleen $\delta^{15}\text{N}$ correspond to the expected migration phenology in gray whales.

46 **ABSTRACT**

47 Individual-level assessments of wild animal health, vital rates, and foraging ecology are critical for
48 understanding population-wide impacts of exposure to stressors. Large whales face multiple stressors,
49 including, but not limited to, ocean noise, pollution, and ship strikes. Because baleen is a continuously
50 growing keratinized structure, serial extraction, and quantification of hormones and stable isotopes
51 along the length of baleen provide a historical record of whale physiology and foraging ecology.
52 Furthermore, baleen analysis enables the investigation of dead specimens, even decades later, allowing
53 comparisons between historic and modern populations. Here, we examined baleen of five sub-adult
54 gray whales and observed distinct patterns of oscillations in $\delta^{15}\text{N}$ values along the length of their baleen
55 plates which enabled estimation of baleen growth rates and differentiation of isotopic niche widths of
56 the whales during winter and summer foraging. In contrast, no clear patterns were apparent in $\delta^{13}\text{C}$
57 values. Prolonged elevation of cortisol in four individuals before death indicate that chronic stress may
58 have impacted their health and survival. Triiodothyronine (T3) increased over months in the whales with
59 unknown causes of death, simultaneous with elevations in cortisol, but both hormones remained stable
60 in the one case of acute death attributed to killer whale predation. This parallel elevation of cortisol and
61 T3 challenges the classic understanding of their interaction and might relate to increased energetic
62 demands during exposure to stressors. Reproductive hormone profiles in subadults did not show cyclical
63 trends, suggesting they had not yet reached sexual maturity. This study highlights the potential of
64 baleen analysis to retrospectively assess gray whales' physiological status, exposure to stressors,
65 reproductive status, and foraging ecology in the months or years leading up to their death, which can be
66 a useful tool for conservation diagnostics to mitigate unusual mortality events.

67 **KEY WORDS:**

68 Mysticetes, stable isotopes, enzyme immunoassays, mortality, longitudinal profiles.

69 **FUNDING:** This project was supported by the Office of Naval Research Marine Mammals and Biology
70 Program (no. N00014-20-1-2760), the Oregon State University Marine Mammal Institute and The John
71 H. Prescott Marine Mammal Rescue Assistance Grant Program provided essential funding for stranding
72 response and tissue collection.

73 **ACKNOWLEDGMENTS:** we are grateful to all personnel and volunteers who assisted with stranding
74 response, necropsy, and collection of specimens.

75 **1. INTRODUCTION**

76 Individual-level assessments of changes in health, vital rates, and foraging ecology of wild
77 animals in response to disturbance events are key for identifying potential impacts on the broader
78 population (Pirodda et al., 2022), as well as gaining insights needed for effective, targeted conservation
79 strategies. Large whales are exposed to an increasing number of stressors, including ocean noise (e.g.,
80 vessel traffic, military sonar, seismic oil and gas exploration, and construction; (Lemos et al., 2022a;
81 Rolland et al., 2012), contaminant, plastic, heavy metal and chemical pollution (Lowe et al., 2022;
82 Reckendorf, 2023; Torres et al., 2023), ship strikes, harmful algal blooms (D'Agostino et al., 2022),
83 entanglement in fishing gear (Clapham, 2016; S. Derville et al., 2023), marine heatwaves (Suryan et al.,
84 2021), and prey shifts (Solène Derville et al., 2023; Pallin et al., 2023; Thomas et al., 2016). Conservation
85 efforts to mitigate threats to whale populations are hindered by challenges of monitoring and repeated
86 sampling due to whales' large size, mobility, and their remote marine habitats (Hunt et al., 2013) and
87 thus constrain assessment of natural and anthropogenic impacts on individual health, vital rates, and
88 foraging ecology.

89 Recently, the use of innovative analytical methods for non-plasma sample types that can be
90 collected from live or dead whales has increased our ability to disentangle different aspects of the
91 complex foraging ecology and physiology of large whales (Fleming et al., 2018; Hunt et al., 2013; Teixeira
92 et al., 2022). Baleen, for example, is a unique structure that forms the filter-feeding apparatus in
93 mysticete whales and is perhaps the best biological tissue for acquiring longitudinal ecological and
94 physiological data, with sufficient temporal resolution to examine seasonal patterns (Caraveo-Patiño et
95 al., 2007; Fernández Ajó et al., 2020, 2018; Hunt et al., 2018). Like other keratinized epidermal tissues
96 (e.g., claws, hair, and spines, whiskers), baleen is a continuously growing structure that extends from a
97 well-vascularized dermal zone. During growth, baleen incorporates the isotopic ratios and endocrine
98 signature of the circulating plasma. The slow growth rate of baleen allows for simultaneous
99 incorporation of the whale's endocrine and stable isotope (SI) history spanning the time of baleen
100 growth. For mysticetes with shorter baleen (e.g., humpback whales, *Megaptera novaeangliae*, and gray
101 whales, *Eschrichtius robustus*), this period is 1–5 years (Caraveo-Patiño et al., 2007a; Lowe et al., 2021b,
102 2021a) versus a decade or more in species with longer baleen (e.g., bowheads, *Balaena mysticetus*)
103 (Hunt et al., 2022, 2017a, 2014; Lysiak et al., 2018). Consequently, paired quantification of hormones
104 and SI values along the longitudinal axis of the baleen plate provides a historical record of the
105 individuals' physiology and insights into their foraging ecology. Notably, baleen is routinely recovered

106 during necropsies, and its inherent strength, durability, and minimal storage requirements (these
107 samples can be preserved dry at room temperature) ensure the preservation of the analytes of interest
108 within the keratin matrix. As a result, detection of hormones and SI's remains feasible in dried samples
109 for decades (Fernández Ajó et al., 2018; Hunt et al., 2017b). These remarkable properties of baleen not
110 only capture multi-year timeframes, enabling the determination of the individuals' seasonal endocrine
111 and foraging patterns, but also facilitates comparisons between historic and modern populations of
112 whales (Fernández Ajó et al., 2020, 2018; Hunt et al., 2018, 2014).

113 Eastern North Pacific (ENP) gray whales migrate between their wintering grounds along the Baja
114 California, Mexico, coastline, and their summer foraging grounds in the Bering, Chukchi, and Beaufort
115 Seas. The ENP population has experienced at least two recorded Unusual Mortality Events (UMEs), in
116 1999-2000 and from 2019 to the present, during which an unusually high number of gray whales were
117 found dead along the Pacific coast from northern Mexico to the Alaskan Arctic, USA. Several factors
118 have been considered as possible causes for the high number of gray whale strandings, including
119 variation in Arctic prey availability and the duration of their feeding season caused by the timing of sea
120 ice formation and breakup (Stewart et al., 2023), starvation, anthropogenically derived toxicants,
121 biotoxins, infectious diseases, parasites, fisheries interactions, and ship strikes (Eguchi et al., 2023;
122 Gulland et al., 2005). In the current UME, dead whales are frequently emaciated, indicating nutritional
123 limitation as a causal factor of death (Christiansen et al., 2021). While poor condition of many of the
124 stranded whales supports the idea that starvation could be a significant contributing factor in these
125 mortalities, the underlying causes of starvation during these events are unknown, and it is also unclear
126 whether the whales' decline in body condition was rapid or gradual.

127 In this study, we analyzed patterns across time of stable isotopes and five hormones within five
128 baleen plates recovered postmortem from five subadult gray whales (4 males, 1 female) that stranded
129 during the 2019-present UME. Our goal is twofold: first, to retrospectively examine the hormone and
130 isotopic profiles in gray whales prior to mortality; and second, to assess potential factors contributing to
131 mortality and the onset timing of chronic illness leading to death. Our isotopic analysis includes the
132 longitudinal profiles of bulk carbon and nitrogen stable isotope ratios in baleen, as they are well-
133 established markers of seasonal diet and foraging grounds in large whales (Best and Schell, 1996;
134 Busquets-Vass et al., 2017; Matthews and Ferguson, 2015). Stable isotopes incorporated into baleen are
135 acquired from an animal's diet, with different prey having characteristic ratios of $^{13}\text{C}/^{12}\text{C}$ and $^{15}\text{N}/^{14}\text{N}$,
136 expressed as $\delta^{13}\text{C}$ and $\delta^{15}\text{N}$, respectively. Predictable enrichment of both $\delta^{13}\text{C}$ and $\delta^{15}\text{N}$ occurs at each

137 trophic level (Kelly, 2000), and additional latitudinal variation in prey isotope ratios often results in
138 annual oscillations in $\delta^{13}\text{C}$ and $\delta^{15}\text{N}$ across the length of whale baleen, reflecting the whales' annual
139 migrations between summering and wintering grounds. For example, $\delta^{15}\text{N}$ values are typically lower
140 when whales consume zooplankton at their summering grounds and are higher when whales are
141 sustained primarily by their own blubber reserves and/or feed on isotopically distinct food on their
142 wintering grounds (Lysiak, 2009). Recent studies have combined stable isotopes with baleen steroid
143 hormone analysis to establish a timeline of tissue growth, allowing interpretation of hormone
144 concentrations over time (e.g., (Hunt et al., 2017a, 2016b, 2014)).

145 Our hormonal analysis quantifies two adrenal glucocorticoid steroids, cortisol and
146 corticosterone, as well as the thyroid hormone triiodothyronine (T3), and two gonadal steroids,
147 progesterone and testosterone. Increased secretion of glucocorticoids from the hypothalamic-pituitary-
148 adrenal (HPA) axis signifies the activation of the vertebrate stress response (Romero and Wingfield,
149 2016). The hypothalamic-pituitary-thyroid axis (HPT) regulates the synthesis and secretion of thyroxine
150 (T4), which subsequently undergoes enzymatic conversion to the more active form, T3. Both T3 and T4
151 modulate basal metabolic rate, growth and development, and thermogenesis, along with other
152 permissive actions (Romero and Wingfield, 2016). Because T3 is generally recognized as the most
153 biologically active thyroid hormone, it has been considered a more relevant biomarker than other forms
154 of the thyroid hormones (Eales, 1988; Flamant et al., 2017). T3 is examined here as a biomarker of
155 nutritional state, i.e., a proxy of foraging success, given its role in regulating metabolic rate in mammals,
156 as reviewed in (Behringer et al., 2018). The two gonadal steroids, progesterone and testosterone, are
157 assessed here as markers of reproductive status. The analysis of reproductive hormones within baleen
158 has proven valuable for assessing pregnancy and inter-calving cycles in females, and testosterone cycles
159 in males, in multiple baleen whale species (Hunt et al., 2022, 2018, 2016b; Lowe et al., 2021b; Lysiak et
160 al., 2023). Here, we examine the reproductive steroids to assess sexual maturity; all our specimens are
161 from subadults, but subadult whales may initiate gonadal secretion of reproductive hormones well in
162 advance of full reproductive competence, and stress is known to delay sexual maturity in many
163 mammals (Dettmer and Chusyd, 2023; Hunt et al., 2022). Further, the individual baselines for each
164 hormone and each individual whale are assessed to monitor individual variability in response to
165 potential stressors.

166 Through the integration of SI and endocrine methodologies, we demonstrate that baleen
167 analysis provides a holistic narrative detailing the health and trophic ecology of individual whales across

168 time, effectively filling knowledge gaps between individual physiology and population impacts.
169 Ultimately, these biomarker techniques can make significant contributions to management and
170 conservation efforts by informing the complex physiological dynamics that underlie whale mortality.

171 **2. MATERIALS & METHODS**

172 **2.1 SAMPLE COLLECTION**

173 From April 2019 to August 2021, a baleen plate from each of five stranded gray whales ($n = 4$
174 males and $n = 1$ female) was collected by the Oregon Marine Mammal Stranding Network (OMMSN,
175 NMFS MMPA/ESA permit No. 18786-06) along the Oregon, USA coast, between Whaleshead Beach in
176 Brookings (42.15°N, -124.35°W) and Cape Mears (45.54°N, -123.96°W). All males had complete baleen
177 plates (i.e., including the most recent growth within the gum), while the female's baleen plate was
178 missing the most recently grown baleen at the root of the baleen plate (i.e., the baleen was cut at the
179 gumline when recovered at necropsy). All specimens were removed from the right side of the rostrum
180 and the center of the rack, where the longest baleen plates are located. The whale's total length (TL,
181 measured as snout-to-fluke-notch), presence of scars, general body condition, and presumed cause of
182 death were also recorded (Table 1). All individuals were classed as "subadults" based on the size
183 categories (i.e., female TL 9–11.7 m, male TL 9–11.1 m; (Rice and Wolman, 1971)), i.e., at least 24
184 months old but not yet sexually mature.

185 **2.2 PREPARATION OF BALEEN PLATES FOR HORMONE EXTRACTION AND QUANTIFICATION**

186 To remove any soft tissues adhered to the base of the baleen plates (proximal end near the gum
187 line with the newest baleen), we rehydrated and softened the tissues by submerging the baleen plates
188 in fresh water, and subsequently scraped the soft tissues off with a metal scraper or scalpel. We then
189 freeze-dried the baleen plates under vacuum (LabConco FreeZone 6L system with Stoppering Tray Dryer,
190 Kansas City, MO, USA), until the pressure reading of the lyophilizer stabilized for at least 12 h, indicating
191 that the samples were dry. Dried, cleaned plates were then stored at room temperature in individual
192 sealed plastic bags, each with a 50 g silica gel desiccant pack (Arbor Assays, Ann Arbor, MI, USA).

193 We collected 20-50 mg of powder from sampling points spaced every 1 cm along the labial edge
194 of the plate, using a hand-held electric rotary grinder (Dremel® model 395 type 5) fitted with a tungsten
195 carbide ball-tip, with each sample collected from a <1.5 cm transverse groove across the posterior face
196 of the plate. The proximal-most point on the base of the baleen plate was designated as the 0 cm point.
197 Sampling started 1 cm from the base and continued every 1 cm to the tip (distal end) until the baleen

198 became too thin to collect the minimum required sample mass for hormone extraction (20 mg); thus,
 199 we typically excluded the distal-most two centimeters of each plate (i.e., the oldest growth). To avoid
 200 cross contamination, during sampling we shielded other regions of the plate with adhesive tape, and
 201 between samples the entire baleen plate, sampling equipment, and fume hood were cleaned with
 202 compressed air, and the work surface and all equipment were also cleaned with 70% ethanol. Powder
 203 samples were weighed to the nearest 0.1 mg on an Ohaus Explorer Pro EP214C analytical balance
 204 (Ohaus, Pine Brook, NJ, USA), with a nearby workstation ionizer (SPI No. 94000, SPIwestek.com) placed
 205 next to the scale to minimize any effects of static electric charge. Weighed samples were placed in 16 ×
 206 100 mm borosilicate glass tubes and securely capped until hormone extraction, which took place within
 207 72 hours of drilling. In total, 110 powder samples were produced, with each whale's plate producing
 208 between 12-27 samples.

209 **Table 1.** Biological information for individual gray whales, *Eschrichtius robustus*, collected along the
 210 Oregon Coast and sampled for both hormone and stable isotope analysis.

Whale Code	Whale ID	Strand Date	Cause of Death	Sex	TL (cm)	Total Samples	BGR (mm/week)	GS (days)	Age Class
Er_1	HMSC_190424_Er	2019-04-24	Unk	F	1080	12*	3.2	~242	Subadult
Er_2	HMSC_200331_Er	2020-03-31	Unk	M	1086	26	3.2	~550	Subadult
Er_3	HMSC_200515_Er	2020-05-15	Unk	M	996	20	3.2	~418	Subadult
Er_4	HMSC_210529_Er	2021-05-29	Unk	M	1060	25	3.2	~528	Subadult
Er_5	HMSC_210816_Er	2021-08-16	Orca	M	1000	27	4.7	~390	Subadult

211 **Cause of death:** Unk = undetermined, Orca = evidence of Killer whale, *Orcinus orca*, predation as acute cause of death; **Sex** = Female (F), Male
 212 (M); **TL** = Total Length from snout to fluke notch in cm; **Total samples** = number of subsamples obtained from each baleen plate; **BGR** = baleen
 213 growth rate estimated in days per cm (from stable isotope analysis); **GS** = Growth span, estimated timespan represented by the entire baleen
 214 plate, in days, derived from baleen growth rate and total length of plate; * only the erupted portion of the baleen was collected during the
 215 necropsy.
 216

217 2.3. STABLE ISOTOPE ANALYSES (SIA)

218 We weighed approximately 1 mg of baleen powder from each sampling location (i.e., every 1 cm
 219 along the longitudinal axis on each baleen plate) directly into tin capsules. Bulk $\delta^{13}\text{C}$ and $\delta^{15}\text{N}$ were
 220 measured using a Thermo FlashSmart elemental analyzer coupled to a Thermo Finnigan Delta Plus XP
 221 continuous-flow isotope ratio mass spectrometer (Thermo Scientific, Bremen, Germany). Results are
 222 expressed in parts per thousand (‰) and delta notation (δ) using the equation: $\delta_{\text{sample}} = [R_{\text{sample}}/R_{\text{standard}} -$
 223 $1] * 1000$, where R_{sample} and R_{standard} are the $^{13}\text{C}/^{12}\text{C}$ or $^{15}\text{N}/^{14}\text{N}$ ratios of the sample and standard,
 224 respectively (Peterson and Fry, 1987). The isotopic reference materials used were supplied by the
 225 International Atomic Energy Agency (IAEA-N-1, $\delta^{15}\text{N} = 0.4 \pm 0.2\text{‰}$; IAEA-CH-7, $\delta^{13}\text{C} = -32.1 \pm 0.05\text{‰}$;

226 IAEA-CH-3, $\delta^{13}\text{C} = -24.7 \pm 0.04\text{‰}$) and the United States Geological Survey (USGS25,
227 $\delta^{13}\text{C} = -34.58 \pm 0.06\text{‰}$, $\delta^{15}\text{N} = -0.94 \pm 0.16\text{‰}$; USGS40, $\delta^{13}\text{C} = -26.3 \pm 0.04\text{‰}$, $\delta^{15}\text{N} = -4.5 \pm 0.1\text{‰}$;
228 USGS41, $\delta^{13}\text{C} = +37.6 \pm 0.04\text{‰}$, $\delta^{15}\text{N} = 47.6 \pm 0.2\text{‰}$);). Internal standards were included with all samples
229 as quality controls; all error data are SD (purified methionine, Alfa Aesar, $\delta^{13}\text{C} = -34.5 \pm 0.06\text{‰}$,
230 $\delta^{15}\text{N} = -0.9 \pm 0.1\text{‰}$; homogenized Chinook salmon muscle, NOAA Auke Bay Laboratories,
231 $\delta^{13}\text{C} = -19.2 \pm 0.05\text{‰}$, $\delta^{15}\text{N} = 15.5 \pm 0.1\text{‰}$). The analytical precision based on the standard deviation of
232 the standard laboratory replicas was $<0.1\text{‰}$ for both $\delta^{13}\text{C}$ and $\delta^{15}\text{N}$. To ensure that our samples did not
233 contain any ^{13}C -depleted lipids, we also measured the C:N ratio of each sub-sample; all of which were
234 within the range expected for pure protein (2.7-3.5) ((Ambrose, 1990); see Supplementary Material,
235 Table S2).

236 **2.4. BALEEN GROWTH RATES AND TIMELINES**

237 To assign an estimated season of growth to each part of the baleen plate, we inspected the $\delta^{15}\text{N}$
238 data for evidence of seasonal changes. Specifically, based on the patterns seen in other baleen whales
239 (Best and Schell, 1996; Lysiak et al., 2018; Matthews and Ferguson, 2015), we assumed that the areas of
240 baleen with lower $\delta^{15}\text{N}$ were grown during summer when whales are most actively foraging, while the
241 regions of baleen with higher $\delta^{15}\text{N}$ were assumed to have grown during winter. Similarly, points with
242 intermediate $\delta^{15}\text{N}$ values (i.e., between summer $\delta^{15}\text{N}$ troughs and winter $\delta^{15}\text{N}$ peaks) were assumed to
243 represent spring and fall migrations. However, because gray whale baleen is relatively short and hence
244 expected to only capture a single full annual cycle, these potential timelines may be imprecise. Thus, we
245 also compared each whale's $\delta^{15}\text{N}$ data to published estimates of baleen growth rate (BGR) for gray
246 whales, which vary from 3.2 mm/week (Sumich, 2001) to 4.7 mm /week (Caraveo-Patiño et al., 2007a).
247 Therefore, for each plate we calculated two potential timelines, counting cm from the base of the
248 baleen plate, using the two published BGR estimates, i.e., assuming the proximal-most point on the
249 plate was grown near the day the whale was found dead, with all other points on the plate then
250 assigned an estimated date of growth based on that BGR (either 3.2 or 4.7 mm/week). These two
251 timelines bracket a range of potential plausible BGRs. The two BGR-derived timelines were then
252 compared to the $\delta^{15}\text{N}$ timeline for that whale, i.e., to verify that our $\delta^{15}\text{N}$ interpretations involve a
253 plausible BGR for this species.

254 **2.5. HORMONE EXTRACTION AND QUANTIFICATION**

255 We extracted hormones from pre-weighed baleen powder samples using 1.6 mL of absolute
256 methanol per 20 mg powder, i.e., keeping a constant ratio of 80:1 mL of solvent to g of sample. This

257 solvent:sample ratio yields good detectability with low variation (inter-sample coefficient of variation <
258 10%; (Fernández Ajó et al., 2022). The solvent:sample mixture was vortexed 2 h at room temperature
259 (Large Capacity Mixer, Glas-Col, Terre Haute, IN, USA; speed set on 40) and centrifuged for 1 min at 4025
260 g. The supernatant from each tube was transferred to individual 13×100 mm borosilicate tubes and
261 dried at 45°C for a minimum of 4 h in a sample evaporator (SpeedVac 121P, Thermo Fisher Scientific,
262 Waltham, MA, USA) under vacuum. We reconstituted the dried samples in 0.50 mL of assay buffer (X065
263 buffer; Arbor Assays, Ann Arbor, MI, USA), sonicated for 5 min, vortexed for 5 min, and transferred the
264 sample to 1.5 mL vapor proof O-ring-capped cryovials. We stored the tubes overnight at –80°C and
265 decanted the extract into a new cryovial the following day. This was considered the "1:1" (full-strength,
266 neat) extract and was stored at -80C until assay.

267 We used commercial enzyme immunoassay (EIA) kits to quantify immunoreactive
268 corticosterone, cortisol, progesterone, testosterone, and T3 in baleen extracts (Arbor Assays kits:
269 corticosterone #K014, cortisol #K003, progesterone #K025, testosterone #K032, and T3 #K056, Ann
270 Arbor, MI, USA). These five kits have previously been validated for gray whale baleen extracts (Hunt et
271 al., 2017b). We assayed all samples at a 1:2 dilution, which in this species produces acceptable
272 detectability and percent-bounds while also allowing assay of multiple hormones from a single 500ul
273 extract. Final data are expressed as ng of hormone per g of dried baleen powder. All assays adhered to
274 standard QA/QC criteria, which included a full standard curve, NSB (non-specific binding), zero dose
275 ("blank"), and an independent control in every EIA microplate. All samples, standards, controls, NSBs,
276 and zeros were assayed in duplicate. Any sample that exhibited a coefficient of variation exceeding 10%
277 between duplicates was re-analyzed. For antibody cross-reactivities, assay sensitivities, and other
278 methodological details, see Hunt et al. (2017a) and the manufacturer's protocols
279 (www.arborassays.com).

280 We evaluated the complete longitudinal profiles for both glucocorticoids, cortisol and
281 corticosterone, in only two individuals (Er_1 and Er_4) to determine the dominant (most abundant)
282 glucocorticoid and to compare the longitudinal profiles of the two hormones. As cortisol was at higher
283 concentration than corticosterone for these two whales, corticosterone was not assayed for the other
284 baleen specimens (see Results). We assayed all other hormones (progesterone, testosterone, T3) for all
285 samples from all whales.

286 **2.6. STATISTICAL ANALYSIS**

287 **2.6.1. HORMONES**

288 All hormone data were log-transformed for data visualization and analyses due to non-normal
289 distribution. We estimated hormone baselines for each gray whale using an iterative process that
290 excludes all data points greater than the mean + two standard deviations until no points exceed this
291 maximum value, following methods from Brown et al., 1988. To test for differences in concentrations of
292 reproductive hormones between sexes, we fit a linear mixed-effects model with random intercepts
293 using the *lme4* R package. All statistical analyses were computed using R (R Development Core Team
294 2023).

295 **2.6.2. STABLE ISOTOPE ANALYSIS**

296 We gauged $\delta^{13}\text{C}$ and $\delta^{15}\text{N}$ fluctuations in baleen plates with a generalized additive model (GAM),
297 fitting a semi-parametric regression with smoothing by cross-validation. We used an ANOVA analysis to
298 test differences in the $\delta^{13}\text{C}$ and $\delta^{15}\text{N}$ values between the phenological phases (wintering vs. summer
299 foraging) utilizing the *aov* function from the stats R package. We then compared the isotopic niche width
300 of each individual gray whale per phenological phase by generating bivariate ellipses in SIBER (Stable
301 Isotope Bayesian Ellipses in R (Jackson et al., 2011), which employs Markov-Chain Monte Carlo (MCMC)
302 simulations to construct parameters of ellipses based on sampling points. We estimated the standard
303 ellipse area corrected for small sample sizes (SEAc , expressed as ‰, which represents the mean core
304 area of each individual's isotopic niche (Jackson et al., 2011; Layman et al., 2007)). We also calculated
305 the Bayesian standard ellipse area (SEAB) to obtain unbiased estimates of the isotopic niche widths
306 (Jackson et al., 2011). To test for significant differences, we ran 20,000 MCMC iterations and constructed
307 95% credible intervals around the mean of each whale. Results are reported as mean \pm standard
308 deviation (SD) unless otherwise stated. All statistical analyses were computed using R (R Development
309 Core Team 2023).

310 **3. RESULTS**

311 **3.1 STUDY ANIMALS, BODY EXAMINATION AND CAUSE OF DEATH.**

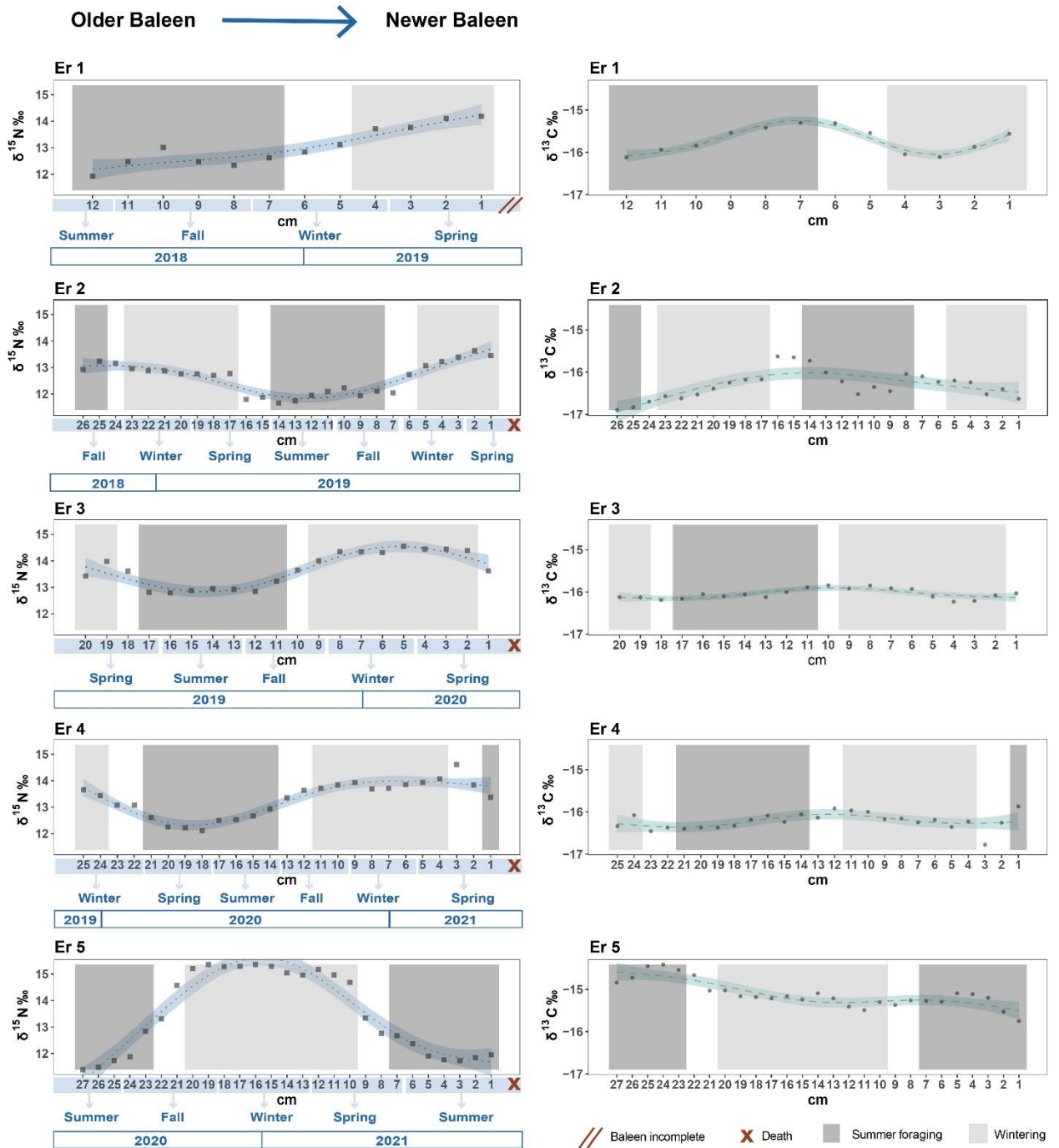
312 All five individuals were in fair to good body condition at necropsy, i.e., no evidence of
313 emaciation. Further, there was no indication that direct human interaction was the cause of death.
314 Notably, all individuals had "rake" mark scars, indicative of physical interactions with killer whales,
315 *Orcinus orca* (Corsi et al., 2022). These scars were primarily observed on the distal end of the fluke and
316 pectoral fins. One individual, HMSC21-08-16-Er (Er 5), presented evidence of acute mortality caused by
317 interactions with killer whales, showing multiple deep and recent "rake" marks on various body parts,

318 particularly the head and flippers, along with extensive and severe hemorrhaging on the top of the
319 head. Cause of death could not be determined for the other four whales.

320 **3.2 ISOTOPIC PATTERNS AND BALEEN GROWTH RATES (BGR)**

321 All baleen plates oscillated in $\delta^{15}\text{N}$ values along their growth axis consistent with expected
322 migration phenology (Figure 1). The growth rate that best fit the expected oscillations with the
323 migration phenology was 3.2 mm/week for all whales except Er_5, for which the best estimate was 4.7
324 mm/week (Figure 1). Excluding Er_1, from which the baleen plate was incomplete (i.e., the proximal-
325 most portion within the gum was missing) we estimate that the baleen of these subadult gray whales
326 recorded around 1.3 years of individual hormone and SI data ($n = 4$; 471.5 ± 68.73 days; Mean \pm SD,
327 Table 1).

328 Mean $\delta^{13}\text{C}$ values were similar among individuals: during wintering, values ranged from -15.2‰
329 $\pm 0.1\text{‰}$ for Er_5, to $-16.3\text{‰} \pm 0.1\text{‰}$ for Er_2; during summer foraging period values ranged from -15.0
330 $\text{‰} \pm 0.4\text{‰}$ for Er_5 to $-16.3\text{‰} \pm 0.4\text{‰}$ for Er_2 (Table 2). Mean $\delta^{13}\text{C}$ values for all individuals were -
331 $15.0\text{‰} \pm 0.4\text{‰}$ and $-15.2\text{‰} \pm 0.1\text{‰}$ for the summer and wintering period, respectively (Figure 2) with no
332 significant differences between these two periods ($F_{(1, 88)} = 1.73$, $p = 0.19$). In contrast, mean $\delta^{15}\text{N}$ values
333 varied among individuals, ranging from $13.0\text{‰} \pm 0.3\text{‰}$ for Er_2 to $15.1\text{‰} \pm 0.2\text{‰}$ for Er_5 during the
334 wintering period to $11.9\text{‰} \pm 0.4\text{‰}$ for the Er_5, to $13.1\text{‰} \pm 0.4\text{‰}$ for the Er_3 during the summer
335 foraging period. The mean $\delta^{15}\text{N}$ values for all individuals was $12\text{‰} \pm 0.4\text{‰}$ and $15.1\text{‰} \pm 0.2\text{‰}$ for the
336 summer foraging and wintering periods, respectively (Figure 2), with a significant difference between
337 periods ($F_{(1, 88)} = 132$, $p < 0.001$).

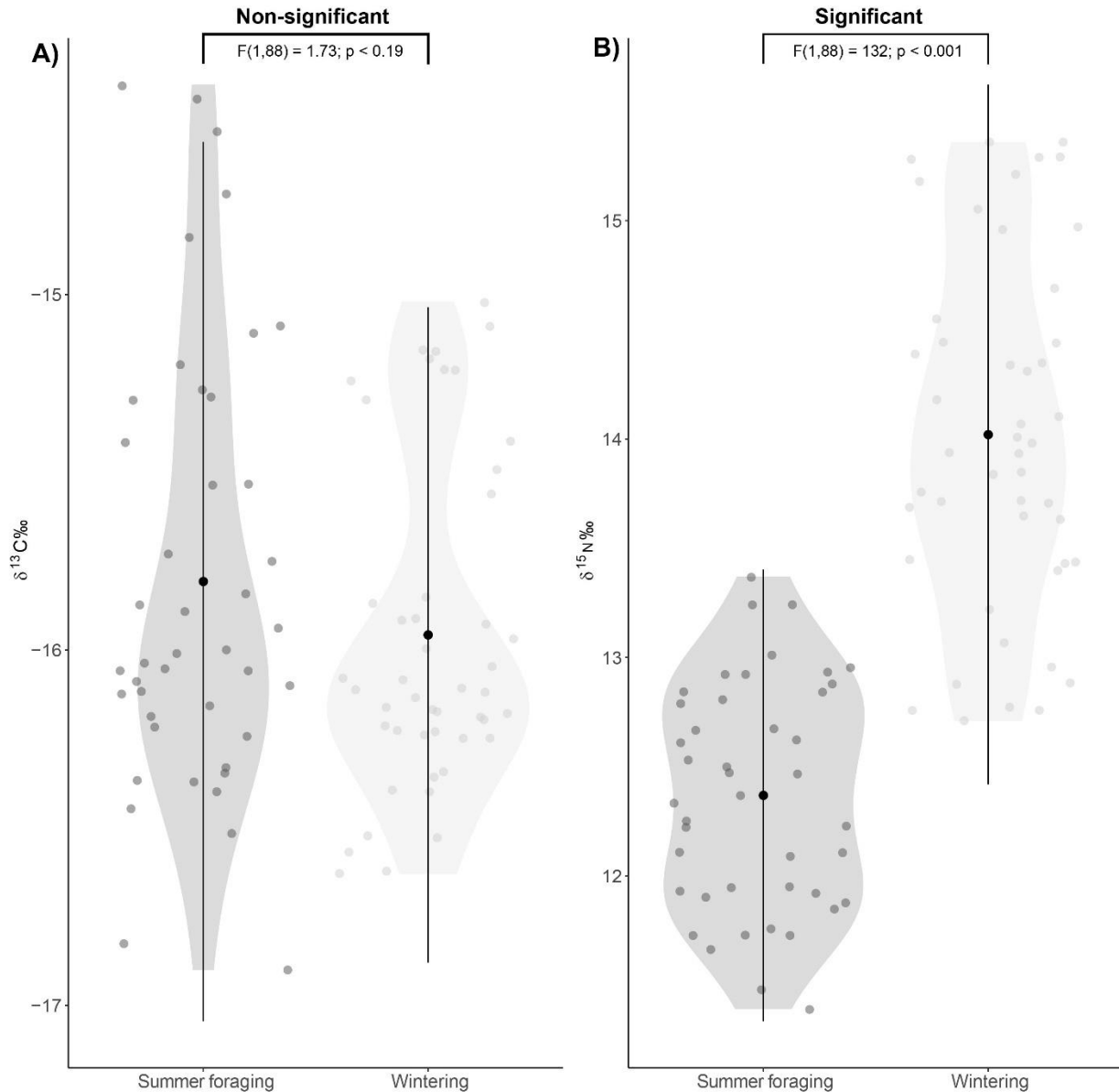


338

339 **Figure 1:** Longitudinal profiles of $\delta^{15}\text{N}$ (left) $\delta^{13}\text{C}$ (right) in baleen plates of stranded subadult gray
 340 whales collected along the Oregon Coast. X-axes show sample location along the baleen, in cm from
 341 base of the baleen plate (i.e., newest baleen = 1 cm), with 1 cm (newest baleen) at far right, i.e., time
 342 runs from left to right. Y-axes show $\delta^{13}\text{C}$ or $\delta^{15}\text{N}$ values (‰). Estimated season and year of growth is
 343 shown below the x-axes, and the time of death is noted with a red X on the x-axis. Migration phenology
 344 is denoted by dark gray (putative summer foraging period) and light gray (putative wintering period)
 345 shading, estimated based on $\delta^{15}\text{N}$ fluctuations. Squares and closed circles depict actual values of $\delta^{15}\text{N}$
 346 and $\delta^{13}\text{C}$, respectively; the dotted and dashed lines depict the fit of the GAM models, with the blue

347 ($\delta^{15}\text{N}$) and green ($\delta^{13}\text{C}$) fringe illustrating the 95% confidence intervals. Only the erupted portion of the
348 baleen plate from Er_1 (top) was available, i.e., the proximal-most portion of the base of the plate was
349 missing, denoted with two parallel red lines on the x-axis.

350



351

352 **Figure 2.** Violin plots for A) $\delta^{13}\text{C}$ and B) $\delta^{15}\text{N}$ values by phenology phase (i.e., summer foraging in dark
353 grey and wintering in light grey). Circles depict actual $\delta^{13}\text{C}$ and $\delta^{15}\text{N}$ values. The black dot represents the
354 mean, and whiskers indicate the standard deviation; statistically significant differences between groups
355 are shown at the top with F and p values from ANOVA.

356

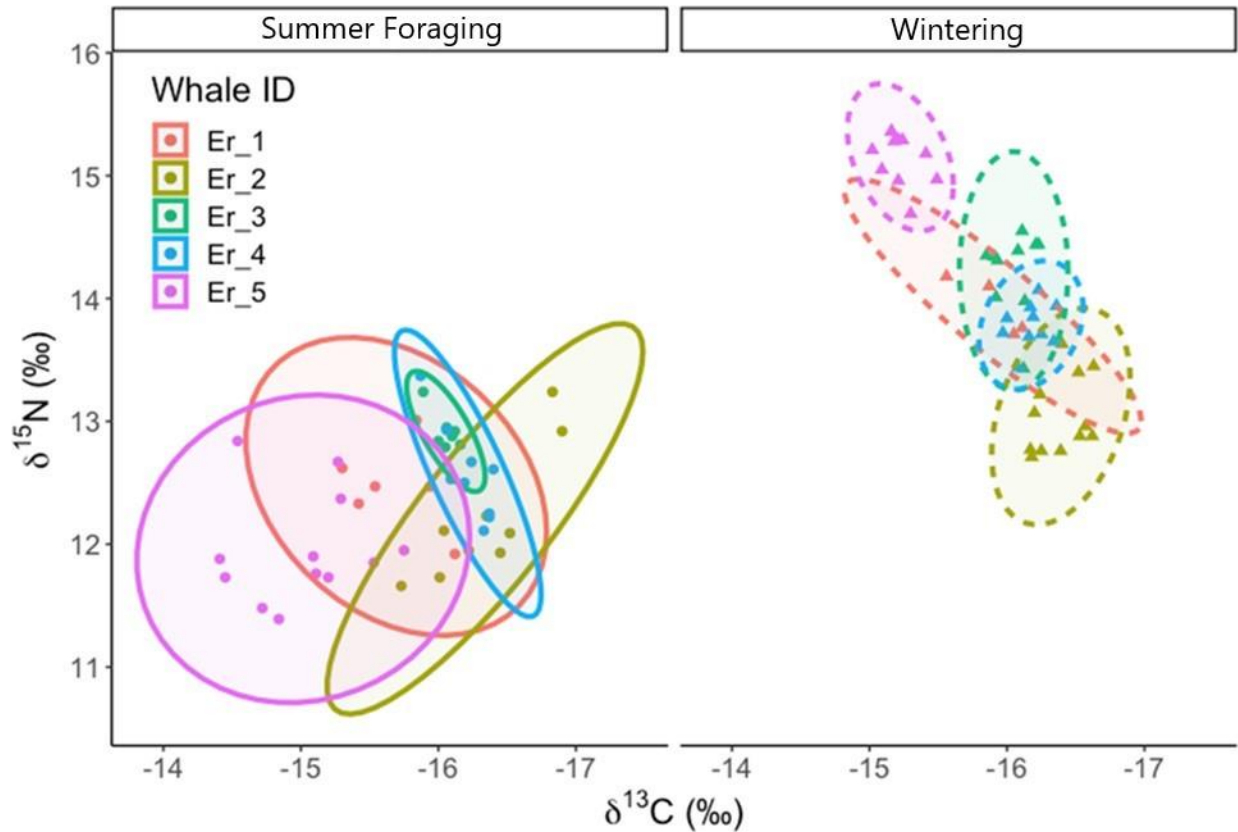
357 The smallest isotopic niche areas for the gray whales were observed during the wintering
358 period, consistent with winter fasting (Figure 3). During winter, Er_4 and Er_5 presented the smallest
standard ellipse areas ($\text{SEA}_C: 0.07\text{‰}^2 / \text{SEA}_B: 0.06\text{‰}^2$ and $\text{SEA}_C: 0.09\text{‰}^2 / \text{SEA}_B: 0.07\text{‰}^2$, respectively) and

359 Er_2 and Er_3 presented the largest standard ellipse areas (SEAc: 0.18‰² / SEAb: 0.16‰² and SEAc:
 360 0.16‰² / SEAc: 0.12‰², respectively). The largest standard ellipse areas of δ¹³C in summer is consistent
 361 with foraging on varied benthic prey in summer with different isotopic compositions (Burnham and
 362 Duffus, 2016a; Nelson et al., 2008a; Newell and Cowles, 2006). During summer foraging, Er_3 and
 363 Er_4 had the smallest standard ellipse areas (SEAc: 0.03‰² / SEAb: 0.02‰² and SEAc: 0.13‰² / SEAb:
 364 0.12‰², respectively) while Er_5 and Er_1 had the largest standard ellipse areas (SEAc: 0.65‰² / SEAb:
 365 0.54‰² and SEAc: 0.43‰² / SEAb: 0.30‰²) (Figure 3; Table 2).

366 **Table 2.** Mean δ¹³C and δ¹⁵N values ± SD for each of the five gray whale baleen plates sampled by season
 367 (summer foraging vs. wintering). Standard ellipse area corrected for small sample sizes (SEAc, expressed
 368 as ‰²), which represents the mean core area of each individual's isotopic niche, and Bayesian standard
 369 ellipse areas (SEAb) with credible intervals (CI).

ID	Summer foraging					Wintering				
	δ ¹³ C (‰)	δ ¹⁵ N (‰)	SEAc (‰ ²)	SEAb (‰ ²)	CI	δ ¹³ C (‰)	δ ¹⁵ N (‰)	SEAc (‰ ²)	SEAb (‰ ²)	CI
Er 1	-15.7 ± 0.3	12.5 ± 0.2	0.43	0.3	(CI: 0.23-0.42)	-15.9 ± 0.2	13.9 ± 0.2	0.12	0.11	(CI: 0.07-0.16)
Er 2	-16.3 ± 0.3	12.2 ± 0.5	0.37	0.38	(CI: 0.30-0.49)	-16.4 ± 0.1	13.0 ± 0.3	0.18	0.16	(CI: 0.13-0.19)
Er 3	-16.0 ± 0.1	13.2 ± 0.4	0.03	0.02	(CI: 0.02-0.04)	-16.1 ± 0.1	14.1 ± 0.4	0.16	0.12	(CI: 0.10-0.16)
Er 4	-16.0 ± 0.1	13.1 ± 0.4	0.13	0.12	(CI: 0.10-0.17)	-16.3 ± 0.1	13.4 ± 0.5	0.07	0.06	(CI: 0.05-0.08)
Er 5	-15.0 ± 0.1	12.0 ± 0.4	0.65	0.54	(CI: 0.46-0.70)	-15.2 ± 0.4	15.1 ± 0.2	0.09	0.07	(CI: 0.06-0.09)

371



372

373 **Figure 3.** $\delta^{13}\text{C}$ and $\delta^{15}\text{N}$ biplot illustrating the isotopic niche width of five subadult gray whales that
 374 stranded along the Oregon Coast, divided by season (Summer foraging vs. wintering). Points within each
 375 ellipse represent sub-samples from each sampled baleen plate, and ellipses represent the estimated
 376 standard ellipse area corrected for small sample sizes (SEAc , expressed as ‰^2).

377 3.4. BALEEN GLUCOCORTICOIDS (CORTISOL AND CORTICOSTERONE)

378 Both glucocorticoids (cortisol & corticosterone) were detectable along the full length of the two
 379 plates for which both hormones were assayed (i.e., Er_1 & Er_4; Figure 4). The longitudinal profiles of
 380 the two hormones generally mirrored each other, with cortisol consistently showing a slightly higher
 381 apparent concentration compared to corticosterone at every sampling point along the baleen
 382 longitudinal axis (Figure 4; electronic supplementary material, Table S1). Therefore, only cortisol was
 383 analyzed for the other three whales. The baseline concentration for cortisol in all individuals fell within
 384 the range of 0.55 ± 0.75 to 11.20 ± 26.66 ng/g (mean \pm SD; Table 3). Among all individuals, except for
 385 Er_5 (the individual presumed to have died acutely due to killer whale predation), there were
 386 pronounced elevations in the apparent concentration of cortisol preceding death (Figure 4). For the
 387 three individuals with unknown cause of death that had complete baleen length (i.e., excluding both
 388 Er_1, missing part of the baleen, and Er_5, known cause of death), the time elapsed from the onset of

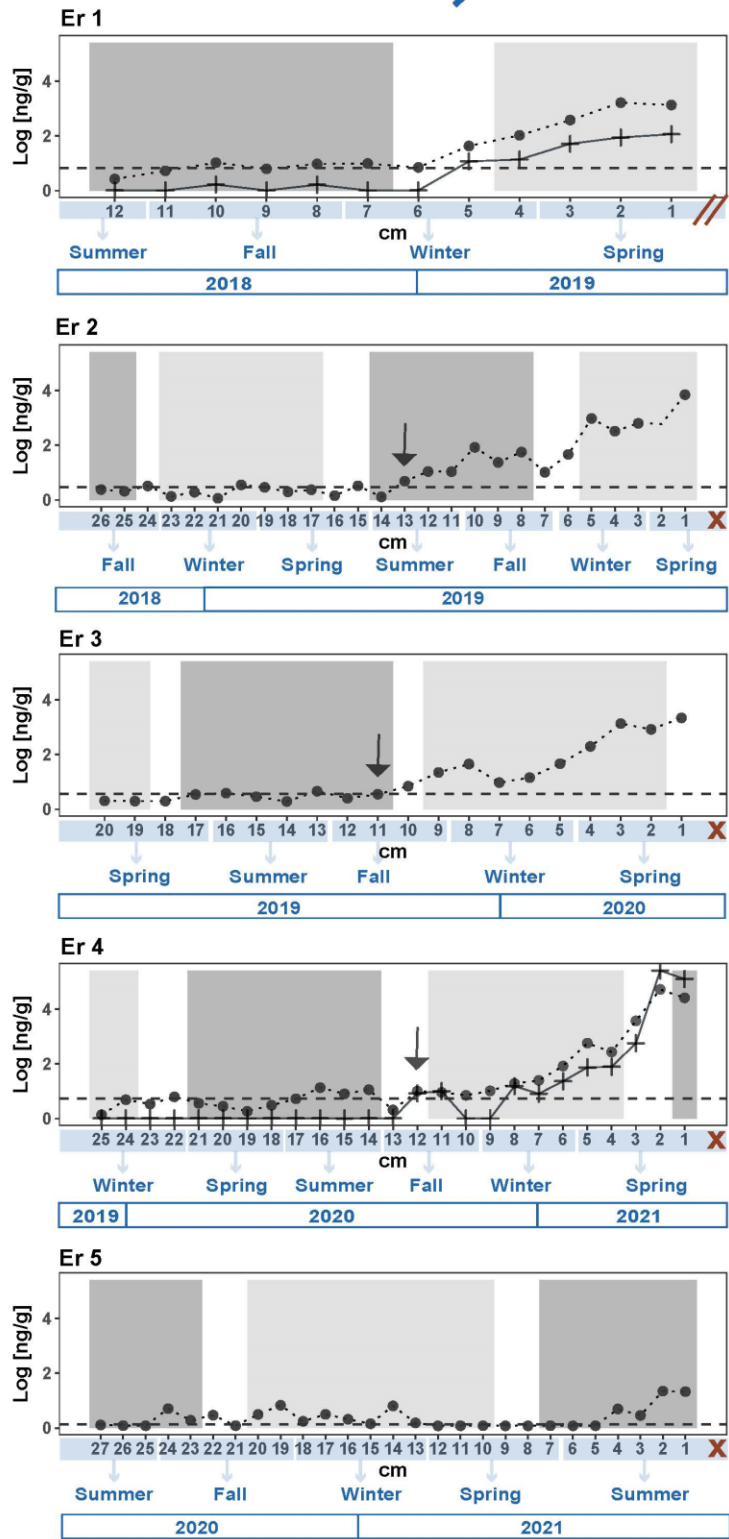
389 the elevation in cortisol to the time of death was estimated to be 284.37 days (13 cm) for Er_2, 240.62
 390 days (11 cm) for Er_3, and 262.50 days (12 cm) for Er_4. On average, this elapsed time was 262.5 days
 391 (approximately 0.72 years).

392 **Table 3.** Individual baselines of gray whale baleen immunoreactive hormone concentrations (expressed
 393 in ng of immunoreactive hormone per g of baleen powder (ng/g)). Baselines are estimated via an
 394 iterative process that excluded all data points greater than the mean + 2SD until no points exceeded this
 395 maximum value (following Brown *et al.*, 1988). Cortisol = immunoreactive baleen cortisol; Progesterone
 396 = immunoreactive baleen progesterone; Testosterone = immunoreactive baleen testosterone; T3 =
 397 immunoreactive baleen triiodothyronine.

ID	Hormone Baselines (ng/g) +/- Standard Deviation			
	Cortisol	Progesterone	Testosterone	T3
Er 1	6.46 +/- 8.29	1.73 +/- 0.64	0.51 +/- 0.25	2.51 +/- 1.15
Er 2	5.19 +/- 9.78	1.39 +/- 1.02	0.38 +/- 0.21	1.66 +/- 1.37
Er 3	4.86 +/- 7.85	2.04 +/- 0.66	0.35 +/- 0.17	1.77 +/- 1.21
Er 4	11.20 +/- 26.66	2.32 +/- 1.08	0.56 +/- 0.34	3.46 +/- 1.44
Er 5	0.55 +/- 0.75	1.46 +/- 0.68	0.39 +/- 0.21	1.88 +/- 0.95

398

Older Baleen \longrightarrow Newer Baleen



Baleen incomplete
 Death
 Log_Corticosterone
 Log_Cortisol

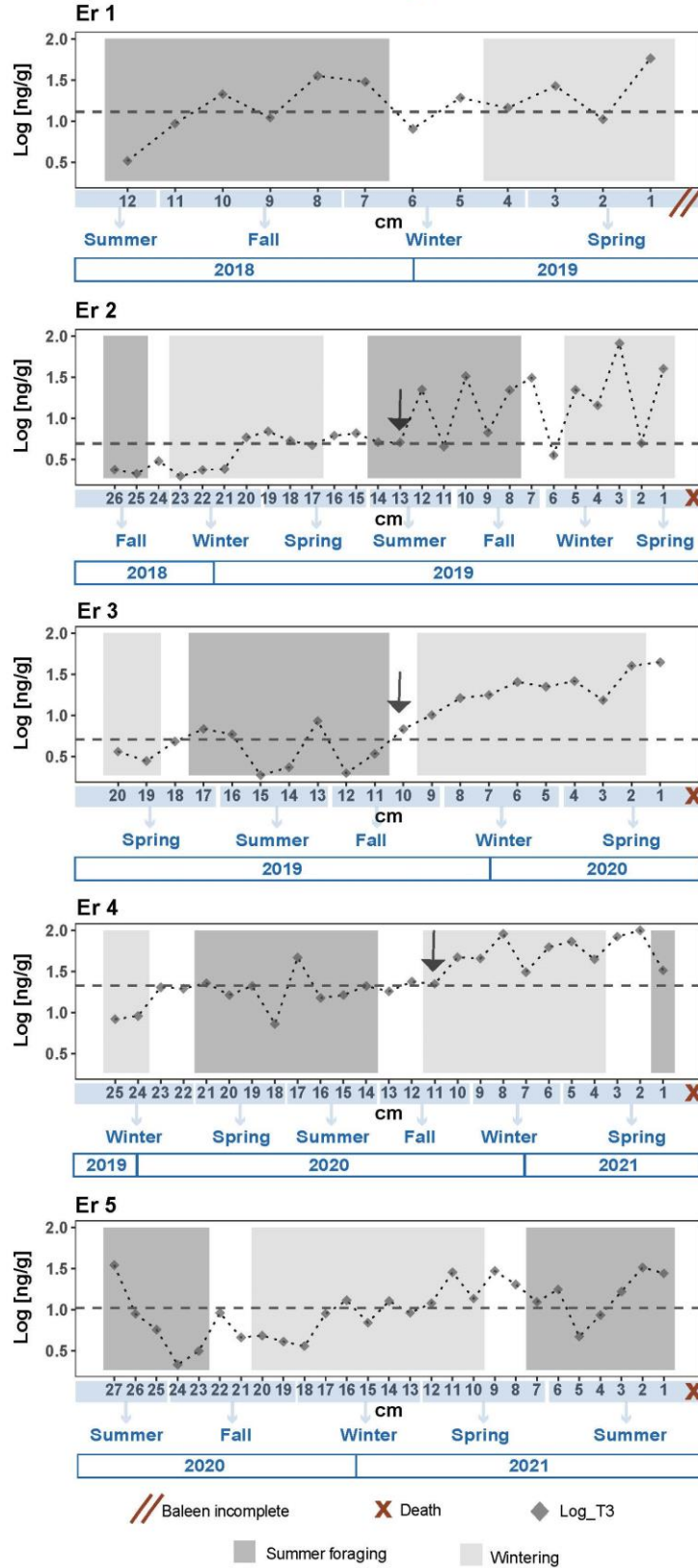
Summer foraging
 Wintering

400 **Figure 4.** Longitudinal profiles of immunoreactive hormone concentrations of corticosterone
401 (Corticosterone; black crosses and dashed line) and cortisol (Cortisol; black circles and dotted line)
402 across the length of baleen plates from five stranded gray whales. The dashed horizontal line indicates
403 the log-transformed baseline for baleen cortisol. X-axes show the location of each sample, in cm from
404 base of the baleen plate (i.e., newest baleen = 1 cm) with y-axes showing concentration of hormone
405 (log-transformed ng of immunoreactive hormone per g of dried baleen powder). Migration phenology is
406 derived from $\delta^{15}\text{N}$ data; dark gray indicates summer foraging and light grey indicates wintering (see
407 Figure 1), and season of growth at each point on the plate was estimated from time of death (noted
408 with a red X on the x-axis). Only the erupted portion of the baleen plate from Er_1 (top) was available,
409 indicated with two parallel red lines on the x-axis. Blue arrows denote the onset of cortisol elevation
410 prior to death.

411 **3.5. TRIIODOTHYRONINE (T3)**

412 Immunoreactive T3 was detectable along the full length of all baleen plates (Figure 5; electronic
413 supplementary material, Table S1). The baseline concentration of T3 ranged from 1.66 ± 1.37 to $3.46 \pm$
414 1.44 ng/g (mean \pm SD; Table 3). Similar to the glucocorticoids, the three individuals with an unknown
415 cause of death that also had a full-length baleen plate (Er_2, Er_3, and Er_4) all had elevated T3
416 preceding death (Figure 5). The onset of the elevation in T3 prior to death was nearly coincident with
417 the timing of elevated cortisol (see Results 3.4).

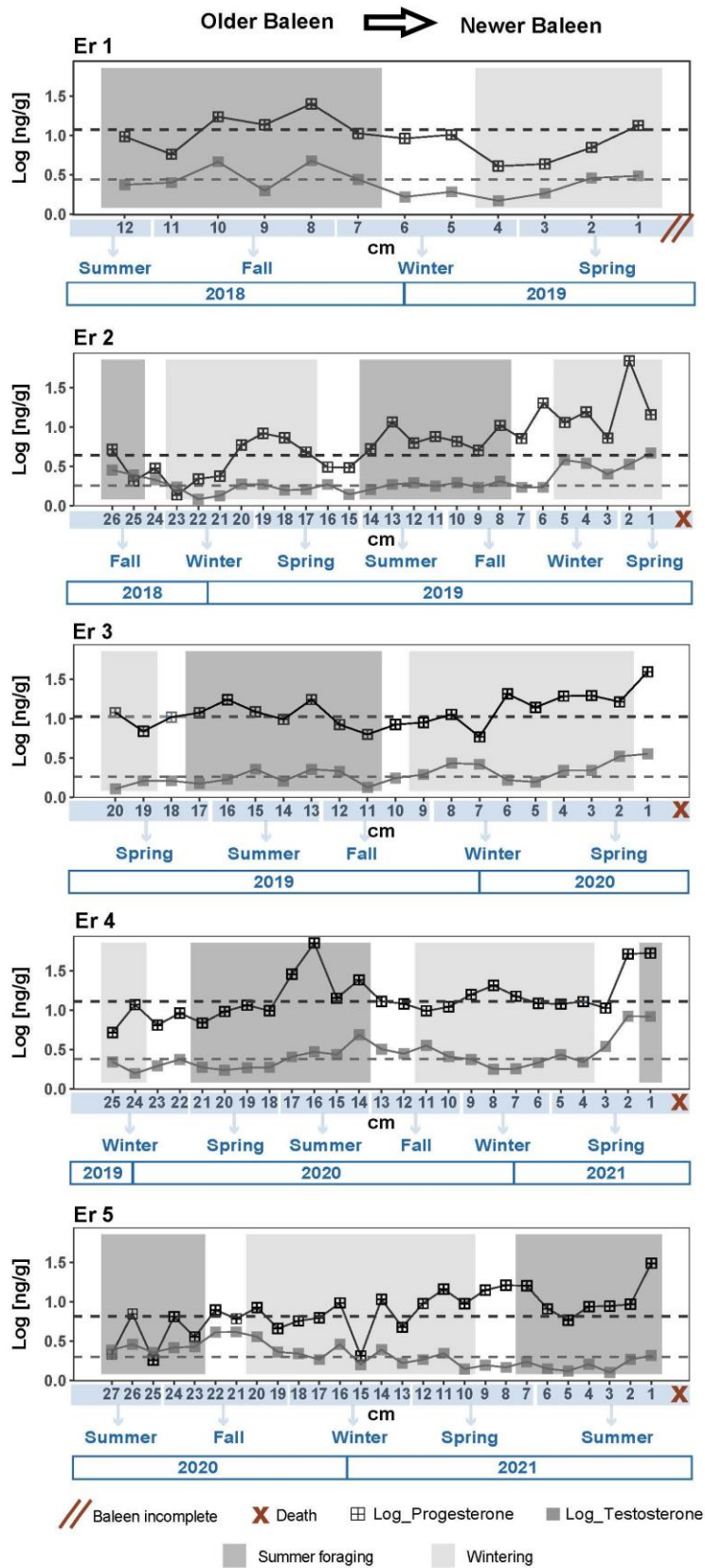
Older Baleen → Newer Baleen



419 **Figure 5.** Longitudinal profiles of immunoreactive hormone concentrations of triiodothyronine (Log_T3;
420 grey rhomboids and dotted line) across the length of baleen plates from five stranded gray whales. The
421 dashed horizontal line indicates the log-transformed baseline for baleen T3. X-axes show the location of
422 each sample, in cm from base of the baleen plate (i.e., newest baleen = 1 cm) with y-axes showing
423 concentration of hormone (log-transformed ng of immunoreactive hormone per g of dried baleen
424 powder). Migration phenology is derived from $\delta^{15}\text{N}$ data; dark gray indicates summer foraging and light
425 grey indicates wintering (see Figure 1), and season of growth at each point on the plate was estimated
426 from time of death (noted with a red X on the x-axis). Only the erupted portion of the baleen plate from
427 Er_1 (top) was available, indicated with two parallel red lines on the x-axis. Blue arrows denote the
428 onset of T3 elevation prior to death.

429 **3.6. REPRODUCTIVE HORMONES (PROGESTERONE AND TESTOSTERONE)**

430 Both progesterone and testosterone were detectable along the full length of the baleen plates
431 (Figure 6; electronic supplementary material, Table S1). The baseline concentration for progesterone in
432 all individuals fell within the range of 1.39 ± 1.02 to 2.32 ± 1.08 ng/g (mean \pm SD; Table 3), and for
433 testosterone the baseline concentration ranged from 0.35 ± 0.17 to 0.56 ± 0.34 ng/g (mean \pm SD; Table
434 3). No significant differences between the two sexes were found in the apparent immunoreactive
435 progesterone and testosterone ($p = 0.9999$).



437 **Figure 6:** Longitudinal profiles of immunoreactive hormone concentrations of progesterone
438 (Progesterone; black cross-square) and testosterone (Testosterone; grey solid squares) across the length
439 of baleen plates from five stranded gray whales. The dashed horizontal lines indicate the log-
440 transformed baseline for baleen progesterone (black) and testosterone (light grey). X-axes show the
441 location of each sample, in cm from base of the baleen plate (i.e., newest baleen = 1 cm) with y-axes
442 showing concentration of hormone (log-transformed ng of immunoreactive hormone per g of dried
443 baleen powder). Migration phenology is derived from $\delta^{15}\text{N}$ data; dark gray indicates summer foraging
444 and light grey indicates wintering (see Figure 1), and season of growth at each point on the plate was
445 estimated from time of death (noted with a red X on the x-axis). Only the erupted portion of the baleen
446 plate from Er_1 (top) was available, indicated with two parallel red lines on the x-axis. Blue arrows
447 denote the onset of T3 elevations prior to death.

448 4. DISCUSSION AND CONCLUSION

449 In this study, we analyzed the SI and hormone profiles in baleen of five sub-adult gray whales,
450 which enabled us to estimate baleen growth rates, distinguish isotopic niche widths during summer and
451 winter periods, and document different endocrinology patterns leading up to death between the whale
452 that died acutely (killer whale attack) and those whales of unknown cause of death. The SI assessment
453 revealed distinct oscillation patterns in $\delta^{15}\text{N}$ values along the baleen plates. The hormone analysis is the
454 first to provide longitudinal profiles of the adrenal, thyroidal, and gonadal axes obtained from the
455 baleen of gray whales in the months leading up to the whales' deaths. Our work demonstrates
456 feasibility of this retrospective approach for gaining insight into gray whale health, physiology, and cause
457 of death.

458 While spatial and temporal variability of stable isotopes in gray whale habitats is still not fully
459 understood (Graham and Bury, 2019; Riekenberg et al., 2021; Trueman and St John Glew, 2019), distinct
460 oscillations in $\delta^{15}\text{N}$ values along the length of subadult gray whale baleen plates allowed us to 1) infer
461 baleen growth rates (which generally agreed with prior estimates (Caraveo-Patiño et al., 2007b; Sumich,
462 2001); and 2) differentiate standard ellipse areas of individuals during summer foraging and wintering
463 locations. The overlap among standard isotopic niche width of the five gray whales during summer
464 suggests either a similar diet across individuals or a diet based on prey species with similar isotopic
465 values. The difference in niche widths between seasons were mostly driven by the low $\delta^{15}\text{N}$ values
466 during summer, likely attributed to the benthic foraging of gray whales on lower trophic level organisms
467 including amphipods (Burnham and Duffus, 2016b), mysids (Newell and Cowles, 2006), crab larvae
468 (Nelson et al., 2008b), shrimps and herring roe (Darling et al., 1998).

469 The larger standard ellipse areas during summer may reflect a diet of a wide range of prey
470 sources in different areas, whereas the smaller standard ellipse areas during winter - mostly driven by

471 high $\delta^{15}\text{N}$ values - are likely related to the fasting period of gray whales during the winter, given that the
472 fasting in mammals is usually associated with increased $\delta^{15}\text{N}$ values due to catabolic or anabolic
473 processes (Fuller et al., 2005; Lee et al., 2012). In accordance with previous reports (Caraveo-Patiño et
474 al., 2007b), there was no distinguishable annual $\delta^{13}\text{C}$ pattern in the gray whale baleen plates. In whale
475 species that migrate between ocean-basins with large gradients in plankton $\delta^{13}\text{C}$, $\delta^{13}\text{C}$ patterns along the
476 baleen reflect seasonal cycles of movements and diet between summer/winter grounds. In bowhead
477 whales, for example, annual oscillations in $\delta^{13}\text{C}$ values are common, presumably resulting from feeding
478 along the whale's annual migratory route that reflects the contrasting geographic isotope values in
479 zooplankton prey found in the Bering (^{13}C -enriched) and Beaufort Seas (^{13}C -depleted) (Saupe et al.,
480 1989; Schell et al., 1989). To better understand the isotopic patterns observed in gray whales and how
481 they reflect the energetic pathways of their summer/winter grounds, future studies may use different
482 analytical approaches including: the use of *isoscapes* (i.e., stable isotope mapping; (Graham and Bury,
483 2019; Trueman and St John Glew, 2019); the combination of bulk and compound-specific amino acid
484 analysis to disentangle the relative contributions of trophic and baseline variation in $\delta^{13}\text{C}$ and $\delta^{15}\text{N}$
485 values (e.g., Riekenberg et al., 2021); and/or integrating isotopic data from prey sources in isotopic
486 mixing models to assess the proportional contribution of each prey sources in their diet.

487 In the glucocorticoid (GC) analyses, we found that both cortisol and corticosterone were
488 detectable along the full length of baleen from two individuals (Er_1 & Er_4), but cortisol was
489 consistently more abundant than corticosterone. Furthermore, corticosterone exhibited similar patterns
490 to cortisol, i.e., corticosterone seemingly did not provide additional information. This pattern generally
491 aligns with traditional assumptions of "cortisol dominance" in mysticetes (primarily based on rare
492 plasma samples from hunted specimens) as well as assumptions that only the more abundant GC need
493 be analyzed, but contrasts with recent findings of more corticosterone than cortisol in baleen of other
494 mysticetes (Fernández Ajó et al., 2018; Hunt et al., 2017a; Lowe et al., 2021a). Most mammals produce
495 both glucocorticoids, and some data indicate the two hormones can respond differently to exogenous
496 stressors, depending on the type and duration of the stressor (Koren et al., 2012). Given our small
497 sample size, we encourage future research on both GCs to further investigate whether they might show
498 species-specific differences or individual differences in glucocorticoid dominance or might provide
499 differing information for acute vs. chronic stressors.

500 Cortisol profiles for the four individuals with unknown cause of death demonstrated a long-term
501 elevation in cortisol that began an estimated 8 months before death. In contrast, the individual known

502 to have died acutely due to killer whale predation (Er_5) had cortisol concentrations that approximate
503 baseline levels across the span of the baleen, suggesting that this individual was in good health before
504 its acute death. These data suggest that the other four individuals experienced a prolonged period of
505 stress. Generally, individual perception of a stressor activates the HPA-axis, leading to an increase in
506 circulating GC levels. Short-term elevations in GCs are thought to aid animals in coping with the stressor
507 (McEwen and Wingfield, 2010; Romero et al., 2009; Romero and Wingfield, 2016), but if the
508 perturbation is severe and/or chronic, the individual deviates from its current life-history stage and
509 enters an “emergency life-history stage”, during which all activities not essential for immediate survival
510 are suppressed (Romero and Wingfield, 2016; Wingfield, 2005; Wingfield et al., 1998). Consequently,
511 chronic elevation of GCs can itself have negative effects on long-term health, through
512 immunosuppression, reduced growth, and inhibition of reproduction (Buck et al., 2007; Dhabhar, 2009,
513 2000; Dhabhar et al., 2012; Kitaysky et al., 1999). Therefore, although the immediate cause of death
514 remains unknown for these four individuals, it is conceivable that the prolonged elevation of cortisol
515 may eventually have directly impacted health and survival, i.e., in addition to any direct negative effects
516 of the stressor itself (Romero and Wingfield, 2016). The presence of “rake marks” attributed to killer
517 whale interactions could provide evidence for increased vulnerability of these individuals. It is plausible
518 that whales undergoing chronic illness might become more susceptible to predation and other threats.

519 T3, like cortisol, tended to show a gradual, months-long increase in the four whales of unknown
520 cause of death (albeit with high individual variability), but remained relatively stable in the whale with
521 an acute cause of death. The simultaneous elevation of both cortisol and T3 was unexpected, as the HPA
522 axis is classically thought to inhibit the HPT axis (Behringer et al., 2018). In fact, elevated GCs in
523 mammals often directly downregulate the HPT axis, resulting in decreases in circulating T3 (Charmandari
524 et al., 2005). However, this downregulation can be temporary (Nicoloff et al., 1970). Further, emerging
525 data indicate that in marine species, T3 may elevate simultaneously with the GCs during those stressors
526 that require increased energetic output, such as swimming while entangled in fishing gear (Hunt et al.,
527 2016a; Lemos et al., 2020; Lysiak et al., 2018). In mammals, T3 can also elevate during thermoregulatory
528 challenges, as elevated T3 directly raises metabolic rate, which elevates body temperature (Behringer et
529 al., 2018; Williams et al., 2019). Indeed, (Lemos et al., 2022b) found that gray whales in poor body
530 condition exhibited higher thyroid hormone concentrations in feces, compared to whales in good body
531 condition, suggesting a possible thermoregulatory influence on T3. In other words, poor body condition
532 in cetaceans entails thinning of the insulative blubber layer and might therefore require a compensatory
533 elevation in metabolic rate and thus an elevation in T3. Similarly, fecal thyroid hormones may reflect

534 changes in food availability (Ayres et al., 2012; Wasser et al., 2017), while psychological/perceptual
535 stressors, i.e., vessel traffic or harassment, are thought to have little impact on T3 levels in whales (Ayres
536 et al., 2012; Fernández Ajó et al., 2020). In our study, all five of our study whales died during the current
537 UME, which generally has been linked to poor nutrition and emaciation (Christiansen et al., 2021).
538 Though it is tempting to ascribe the gradual elevation in T3 seen here to the poor body condition
539 reported in gray whales during the UME generally, the necropsy reports of these five individuals did not
540 describe severe emaciation. However, it is possible that these whales were in relatively lower body
541 condition with respect to the population mean. Overall, we speculate that whales in poor body
542 condition may elevate T3 in response to thermoregulatory demands. This hypothesis could be tested
543 with further comparisons of baleen from stranded whales in poor vs. good body condition, ideally with
544 measurements of body condition, e.g., blubber thickness or body area index derived from drone-based
545 photogrammetry (Bierlich et al., 2021; Burnett et al., 2019). Finally, T3 also commonly varies across life
546 history stages (Wilsterman et al., 2015), and thus studies of T3 patterns in baleen of juveniles as
547 compared to adults may be informative.

548 We also quantified reproductive hormones across the baleen's entire length in four subadult
549 males and one subadult female. To our knowledge, these are the first longitudinal profiles of
550 reproductive hormones from gray whales across a full calendar year. As expected for this reproductive
551 age class (subadults), we did not observe temporal patterns, cyclical trends, or elevated hormone
552 concentrations, suggesting none of the subadults had yet reached sexual maturity. Nevertheless, our
553 results add to knowledge about expected baselines of reproductive hormones in subadults and may thus
554 inform future efforts to identify onset of sexual maturity. Our results also underscore the potential to
555 capture at least one year of information from adult gray whale baleen, as there have been uncertainties
556 about the feasibility of capturing complete pregnancies or multiple pregnancies within gray whale
557 baleen (max baleen length ~30 cm), or whether seasonal testosterone cyclicity in males could be
558 discerned. Our subadult baleen specimens captured an estimated timeframe of 1.3 years. Further, adult
559 baleen generally captures a longer timespan than subadult baleen (since subadults not only might have
560 shorter baleen but also tend to have faster baleen growth rate); thus, these results suggest that adult
561 gray whale baleen may capture a sufficient timeframe to examine at least one if not two prior
562 reproductive cycles.

563 The ENP gray whale population has rebounded from a dramatic decline attributed to whaling
564 from less than 4,000 by 1900 to a peak abundance estimated at 26,916 individuals (Stewart and Weller,

2021; Swartz et al., 2006). However, the ENP gray whale population has exhibited significant fluctuations, marked by two Unusual Mortality Events (UMEs) that curtailed population size, underscoring the susceptibility of gray whales to oceanic conditions, resource availability, and other influences (Torres et al., 2022). The occurrence of recurrent UMEs with often-unknown causes in the ENP gray whale population highlights the necessity for innovative methodologies to investigate and better understand the causes of death and physiological response of individuals to fluctuations in the environment. Despite the characteristic shorter length of gray whale baleen compared to other mysticete species, and thus the relatively brief period of longitudinal data that can be inferred, even subadult gray whale baleen captures a >1 year timespan, and adult baleen specimens may capture a longer timeframe. In sum, baleen analysis in gray whales allows assessment of physiological status of at least the past year and may enable inferences as to the cause of death (acute vs. chronic, nutritional vs. non-nutritional stress). Overall, baleen analysis has emerged as powerful tool that enables a comprehensive and retrospective assessment of gray whale hormonal profiles, stress responses, reproductive status, and foraging ecology in the months or years leading up to their death.

5. REFERENCES

- Ambrose, S.H., 1990. Preparation and characterization of bone and tooth collagen for isotopic analysis. *J Archaeol Sci* 17, 431–451. [https://doi.org/10.1016/0305-4403\(90\)90007-R](https://doi.org/10.1016/0305-4403(90)90007-R)
- Ayres, K.L., Booth, R.K., Hempelmann, J.A., Koski, K.L., Emmons, C.K., Baird, R.W., Balcomb-Bartok, K., Hanson, M.B., Ford, M.J., Wasser, S.K., 2012. Distinguishing the impacts of inadequate prey and vessel traffic on an endangered killer whale (*Orcinus orca*) population. *PLoS One* 7. <https://doi.org/10.1371/journal.pone.0036842>
- Behringer, V., Deimel, C., Hohmann, G., Negrey, J., Schaebs, F.S., Deschner, T., 2018. Applications for non-invasive thyroid hormone measurements in mammalian ecology, growth, and maintenance. *Horm Behav* 105, 66–85. <https://doi.org/10.1016/j.yhbeh.2018.07.011>
- Best PB, Schell DM. 1996. Stable isotopes in southern right whale (*Eubalaena australis*) baleen as indicators of seasonal movements, feeding and growth. *Marine Biology* 124:483-94.
- Bierlich, K.C., Hewitt, J., Bird, C.N., Schick, R.S., Friedlaender, A., Torres, L.G., Dale, J., Goldbogen, J., Read, A.J., Calambokidis, J., Johnston, D.W., 2021. Comparing uncertainty associated with 1-, 2-, and 3d aerial photogrammetry-based body condition measurements of baleen whales. *Front Mar Sci* 8. <https://doi.org/10.3389/fmars.2021.749943>

595 Brown, J.L., Goodrowe, K.L., Simmons, L.G., Armstrong, D.L., Wildt, D.E., 1988. Evaluation of the
596 pituitary-gonadal response to GnRH, and adrenal status, in the leopard (*Panthera pardus*
597 *japonensis*) and tiger (*Panthera tigris*). *Reproduction* 82, 227–236.
598 <https://doi.org/10.1530/jrf.0.0820227>

599 Buck, C.L., O'Reilly, K.M., Kildaw, S.D., 2007. Interannual variability of Black-legged Kittiwake productivity
600 is reflected in baseline plasma corticosterone. *Gen Comp Endocrinol* 150.
601 <https://doi.org/10.1016/j.ygcen.2006.10.011>

602 Burnett, J.D., Lemos, L., Barlow, D., Wing, M.G., Chandler, T., Torres, L.G., 2019. Estimating
603 morphometric attributes of baleen whales with photogrammetry from small UASs: A case study
604 with blue and gray whales. *Mar Mamm Sci* 35. <https://doi.org/10.1111/mms.12527>

605 Burnham, R.E., Duffus, D.A., 2016a. Gray Whale (*Eschrichtius robustus*) predation and the demise of
606 amphipod prey reserves in Clayoquot Sound, British Columbia. *Aquat Mamm* 42, 123–126.
607 <https://doi.org/10.1578/AM.42.2.2016.123>

608 Busquets-Vass, G., Newsome, S.D., Calambokidis, J., Serra-Valente, G., Jacobsen, J.K., Aguíñiga-García, S.,
609 Gendron, D., 2017. Estimating blue whale skin isotopic incorporation rates and baleen growth
610 rates: Implications for assessing diet and movement patterns in mysticetes. *PLoS One* 12.
611 <https://doi.org/10.1371/journal.pone.0177880>

612 Caraveo-Patiño, J., Hobson, K.A., Soto, L.A., 2007b. Feeding ecology of gray whales inferred from stable-
613 carbon and nitrogen isotopic analysis of baleen plates. *Hydrobiologia* 586, 17–25.
614 <https://doi.org/10.1007/s10750-006-0477-5>

615 Charmandari, E., Tsigos, C., Chrousos, G., 2005. Endocrinology of the stress response. *Annu Rev Physiol*
616 67, 259–284. <https://doi.org/10.1146/annurev.physiol.67.040403.120816>

617 Christiansen, F., Rodríguez-González, F., Martínez-Aguilar, S., Urbán, J., Swartz, S., Warick, H., Vivier, F.,
618 Bejder, L., 2021. Poor body condition associated with an unusual mortality event in gray whales.
619 *Mar Ecol Prog Ser* 658, 237–252. <https://doi.org/10.3354/meps13585>

620 Clapham, P., 2016. Managing Leviathan: conservation challenges for the great whales in a post-whaling
621 world. *Oceanography* 29, 214–225. <https://doi.org/10.5670/oceanog.2016.70>

622 Corsi, E., Calambokidis, J., Flynn, K.R., Steiger, G.H., 2022. Killer whale predatory scarring on mysticetes:
623 A comparison of rake marks among blue, humpback, and gray whales in the eastern North Pacific.
624 *Mar Mamm Sci* 38, 223–234. <https://doi.org/10.1111/mms.12863>

625 D’Agostino, V.C., Fernández Ajó, A., Degradi, M., Krock, B., Hunt, K.E., Uhart, M.M., Buck, C.L., 2022.
626 Potential endocrine correlation with exposure to domoic acid in Southern Right Whale (*Eubalaena*
627 *australis*) at the Península Valdés breeding ground. *Oecologia* 198, 21–34.
628 <https://doi.org/10.1007/s00442-021-05078-4>

629 Darling, J.D., Keogh, K.E., Steeves, T.E., 1998. GRAY WHALE (*Eschrichtius robustus*) habitat utilization and
630 prey species off Vancouver island, B. C. *Mar Mamm Sci* 14, 692–720.
631 <https://doi.org/10.1111/j.1748-7692.1998.tb00757.x>

632 Derville, S., Buell, T.V., Corbett, K.C., Hayslip, C., Torres, L.G., 2023. Exposure of whales to entanglement
633 risk in Dungeness crab fishing gear in Oregon, USA, reveals distinctive spatio-temporal and climatic
634 patterns. *Biol Conserv* 281, 109989. <https://doi.org/10.1016/j.biocon.2023.109989>

635 Derville, Solène, Torres, L.G., Newsome, S.D., Somes, C.J., Valenzuela, L.O., Vander Zanden, H.B., Baker,
636 C.S., Bérubé, M., Busquets-Vass, G., Carlyon, K., Childerhouse, S.J., Constantine, R., Dunshea, G.,
637 Flores, P.A.C., Goldsworthy, S.D., Graham, B., Groch, K., Gröcke, D.R., Harcourt, R., Hindell, M.A.,
638 Hulva, P., Jackson, J.A., Kennedy, A.S., Lundquist, D., Mackay, A.I., Neveceralova, P., Oliveira, L.,
639 Ott, P.H., Palsbøll, P.J., Patenaude, N.J., Rowntree, V., Sironi, M., Vermeulen, E., Watson, M.,
640 Zerbini, A.N., Carroll, E.L., 2023. Long-term stability in the circumpolar foraging range of a Southern
641 Ocean predator between the eras of whaling and rapid climate change. *Proceedings of the*
642 *National Academy of Sciences* 120. <https://doi.org/10.1073/pnas.2214035120>

643 Dettmer, A.M., Chusyd, D.E., 2023. Early life adversities and lifelong health outcomes: A review of the
644 literature on large, social, long-lived nonhuman mammals. *Neurosci Biobehav Rev* 152, 105297.
645 <https://doi.org/10.1016/j.neubiorev.2023.105297>

646 Dhabhar, F.S., 2009. Enhancing versus suppressive effects of stress on immune function: implications for
647 immunoprotection and immunopathology. *Neuroimmunomodulation* 16, 300–317.
648 <https://doi.org/10.1159/000216188>

649 Dhabhar, F.S., 2000. Acute stress enhances while chronic stress suppresses skin immunity: the role of
650 stress hormones and leukocyte trafficking. *Ann N Y Acad Sci* 917, 876–893.
651 <https://doi.org/10.1111/j.1749-6632.2000.tb05454.x>

652 Dhabhar, F.S., Malarkey, W.B., Neri, E., McEwen, B.S., 2012. Stress-induced redistribution of immune
653 cells—From barracks to boulevards to battlefields: A tale of three hormones – Curt Richter Award
654 Winner. *Psychoneuroendocrinology* 37, 1345–1368.
655 <https://doi.org/10.1016/j.psyneuen.2012.05.008>

656 Eales, J.G., 1988. The influence of nutritional state on thyroid function in various vertebrates. *Am Zool*
657 28, 351–362. <https://doi.org/10.1093/icb/28.2.351>

658 Eguchi, T., Lang, A.R., Weller, D.W., 2023. NOAA Technical Memorandum NMFS Eastern north pacific
659 gray whale calf production 1994-2023. <https://doi.org/10.25923/e9at-x936>

660 Fernández Ajó, A., Hunt, K.E., Dillon, D., Uhart, M., Sironi, M., Rowntree, V., Loren Buck, C., 2022.
661 Optimizing hormone extraction protocols for whale baleen: Tackling questions of solvent:sample
662 ratio and variation. *Gen Comp Endocrinol* 315, 113828.
663 <https://doi.org/10.1016/j.ygcen.2021.113828>

664 Fernández Ajó, A.A., Hunt, K.E., Giese, A.C., Sironi, M., Uhart, M., Rowntree, V.J., Marón, C.F., Dillon, D.,
665 DiMartino, M., Buck, C.L., 2020. Retrospective analysis of the lifetime endocrine response of
666 southern right whale calves to gull wounding and harassment: A baleen hormone approach. *Gen*
667 *Comp Endocrinol* 296, 113536. <https://doi.org/10.1016/j.ygcen.2020.113536>

668 Fernández Ajó, A.A., Hunt, K.E., Uhart, M., Rowntree, V., Sironi, M., Marón, C.F., Di Martino, M., Buck,
669 C.L., 2018. Lifetime glucocorticoid profiles in baleen of right whale calves: potential relationships to
670 chronic stress of repeated wounding by Kelp Gulls. *Conserv Physiol* 6, 1–12.
671 <https://doi.org/10.1093/conphys/coy045>

672 Flamant, F., Cheng, S.Y., Hollenberg, A.N., Moeller, L.C., Samarut, J., Wondisford, F.E., Yen, P.M.,
673 Refetoff, S., 2017. Thyroid hormone signaling pathways: Time for a more precise nomenclature.
674 *Endocrinology*. <https://doi.org/10.1210/en.2017-00250>

675 Fleming, A.H., Kellar, N.M., Allen, C.D., Kurle, C.M., 2018. The utility of combining stable isotope and
676 hormone analyses for marine megafauna research. *Front Mar Sci* 5.
677 <https://doi.org/10.3389/fmars.2018.00338>

678 Fuller, B.T., Fuller, J.L., Sage, N.E., Harris, D.A., O'Connell, T.C., Hedges, R.E.M., 2005. Nitrogen balance
679 and $\delta^{15}\text{N}$: Why you're not what you eat during nutritional stress. *Rapid Communications in Mass*
680 *Spectrometry* 19. <https://doi.org/10.1002/rcm.2090>

681 Graham, B., Bury, S., 2019. Marine Isoscapes for trophic and animal movement studies in the southwest
682 Pacific Ocean, New Zealand Aquatic Environment and Biodiversity Report No. 2018.

683 Gulland, F., Pérez-Cortés, H., Urbán, J.R., Rojas-Bracho, L., Ylitalo, G., Weir, J., Norman, S., Muto, M.,
684 Rugh, D., Kreuder, C., Rowles, T., 2005. Eastern North Pacific gray whale (*Eschrichtius robustus*)
685 unusual mortality event, 1999-2000. U.S. Department of Commerce. NOAA Technical
686 Memorandum. NMFS-AFSC-150. 33 pp.

687 Hunt, K.E., Buck, C.L., Ferguson, S.H., Fernández Ajo, A., Heide-Jørgensen, M.P., Matthews, C.J.D., 2022.
688 Male bowhead whale reproductive histories inferred from baleen testosterone and stable
689 isotopes. *Integrative Organismal Biology* 4. <https://doi.org/10.1093/iob/obac014>

690 Hunt, K.E., Innis, C.J., Merigo, C., Rolland, R.M., 2016a. Endocrine responses to diverse stressors of
691 capture, entanglement and stranding in leatherback turtles (*Dermochelys coriacea*). *Conserv*
692 *Physiol* 4, cow022. <https://doi.org/10.1093/conphys/cow022>

693 Hunt, K.E., Lysiak, N.S., Moore, M., Rolland, R.M., 2017a. Multi-year longitudinal profiles of cortisol and
694 corticosterone recovered from baleen of North Atlantic right whales (*Eubalaena glacialis*). *Gen*
695 *Comp Endocrinol* 254, 50–59. <https://doi.org/10.1016/j.ygcen.2017.09.009>

696 Hunt, K.E., Lysiak, N.S., Moore, M.J., Rolland, R.M., 2016b. Longitudinal progesterone profiles in baleen
697 from female North Atlantic right whales (*Eubalaena glacialis*) match known calving history.
698 *Conserv Physiol* 4, cow014. <https://doi.org/10.1093/conphys/cow014>

699 Hunt, K.E., Lysiak, N.S., Robbins, J., Moore, M.J., Seton, R.E., Torres, L., Loren Buck, C., Buck, C.L., 2017b.
700 Multiple steroid and thyroid hormones detected in baleen from eight whale species. *Conserv*
701 *Physiol* 5. <https://doi.org/10.1093/conphys/cox061>

702 Hunt, K.E., Lysiak, N.S.J., Matthews, C.J.D., Lowe, C., Fernández Ajó, A., Dillon, D., Willing, C., Heide-
703 Jørgensen, M.P., Ferguson, S.H., Moore, M.J., Buck, C.L., 2018. Multi-year patterns in testosterone,
704 cortisol and corticosterone in baleen from adult males of three whale species. *Conserv Physiol* 6,
705 1–16. <https://doi.org/10.1093/conphys/coy049>

706 Hunt, K.E., Moore, M.J., Rolland, R.M., Kellar, N.M., Hall, A.J., Kershaw, J., Raverty, S.A., Davis, C.E.,
707 Yeates, L.C., Fauquier, D.A., Rowles, T.K., Kraus, S.D., 2013. Overcoming the challenges of studying
708 conservation physiology in large whales: a review of available methods. *Conserv Physiol* 1, cot006–
709 cot006. <https://doi.org/10.1093/conphys/cot006>

710 Hunt, K.E., Stimmelmayer, R., George, C., Hanns, C., Suydam, R., Brower, H., Rolland, R.M., 2014. Baleen
711 hormones: a novel tool for retrospective assessment of stress and reproduction in bowhead
712 whales (*Balaena mysticetus*). *Conserv Physiol* 2, cou030–cou030.
713 <https://doi.org/10.1093/conphys/cou030>

714 Jackson, A.L., Inger, R., Parnell, A.C., Bearhop, S., 2011. Comparing isotopic niche widths among and
715 within communities: SIBER - Stable Isotope Bayesian Ellipses in R. *Journal of Animal Ecology* 80,
716 595–602. <https://doi.org/10.1111/j.1365-2656.2011.01806.x>

717 Kelly, J.F., 2000. Stable isotopes of carbon and nitrogen in the study of avian and mammalian trophic
718 ecology. *Can J Zool* 78, 1–27. <https://doi.org/10.1139/z99-165>

719 Kitaysky, A.S., Wingfield, J.C., Piatt, J.F., 1999. Dynamics of food availability, body condition and
720 physiological stress response in breeding Black-legged Kittiwakes. *Funct Ecol* 13, 577–584.
721 <https://doi.org/10.1046/j.1365-2435.1999.00352.x>

722 Koren, L., Whiteside, D., Fahlman, Å., Ruckstuhl, K., Kutz, S., Checkley, S., Dumond, M., Wynne-Edwards,
723 K., 2012. Cortisol and corticosterone independence in cortisol-dominant wildlife. *Gen Comp*
724 *Endocrinol* 177. <https://doi.org/10.1016/j.ygcen.2012.02.020>

725 Layman, C.A., Arrington, D.A., Montaña, C.G., Post, D.M., 2007. Can stable isotope ratios provide for
726 community-wide measures of trophic structure? *Ecology* 88, 42–48. [https://doi.org/10.1890/0012-9658\(2007\)88\[42:CSIRPF\]2.0.CO;2](https://doi.org/10.1890/0012-9658(2007)88[42:CSIRPF]2.0.CO;2)

727

728 Lee, T.N., Buck, C.L., Barnes, B.M., O'Brien, D.M., 2012. A test of alternate models for increased tissue
729 nitrogen isotope ratios during fasting in hibernating arctic ground squirrels. *Journal of*
730 *Experimental Biology*. <https://doi.org/10.1242/jeb.068528>

731 Lemos, L.S., Haxel, J.H., Olsen, A., Burnett, J.D., Smith, A., Chandler, T.E., Nieukirk, S.L., Larson, S.E., Hunt,
732 K.E., Torres, L.G., 2022a. Effects of vessel traffic and ocean noise on gray whale stress hormones.
733 *Sci Rep* 12. <https://doi.org/10.1038/s41598-022-14510-5>

734 Lemos, L.S., Olsen, A., Smith, A., Burnett, J.D., Chandler, T.E., Larson, S., Hunt, K.E., Torres, L.G., 2022b.
735 Stressed and slim or relaxed and chubby? A simultaneous assessment of gray whale body condition
736 and hormone variability. *Mar Mamm Sci* 38, 801–811. <https://doi.org/10.1111/mms.12877>

737 Lemos, L.S., Olsen, A., Smith, A., Chandler, T.E., Larson, S., Hunt, K., Torres, L.G., 2020. Assessment of
738 fecal steroid and thyroid hormone metabolites in eastern North Pacific gray whales. *Conserv*
739 *Physiol* 8. <https://doi.org/10.1093/conphys/coaa110>

740 Lowe, C.L., Hunt, K.E., Robbins, J., Seton, R.E., Rogers, M., Gabriele, C.M., Neilson, J.L., Landry, S.,
741 Teerlink, S.S., Buck, C.L., 2021a. Patterns of cortisol and corticosterone concentrations in
742 humpback whale (*Megaptera novaeangliae*) baleen are associated with different causes of death.
743 *Conserv Physiol* 9. <https://doi.org/10.1093/conphys/coab096>

744 Lowe, C.L., Hunt, K.E., Rogers, M.C., Neilson, J.L., Robbins, J., Gabriele, C.M., Teerlink, S.S., Seton, R.,
745 Buck, C.L., 2021b. Multi-year progesterone profiles during pregnancy in baleen of humpback
746 whales (*Megaptera novaeangliae*). *Conserv Physiol* 9. <https://doi.org/10.1093/conphys/coab059>

747 Lowe, C.L., Jordan-Ward, R., Hunt, K.E., Rogers, M.C., Werth, A.J., Gabriele, C., Neilson, J., von Hippel,
748 F.A., Buck, C.L., 2022. Case studies on longitudinal mercury content in humpback whale
749 (*Megaptera novaeangliae*) baleen. *Heliyon* 8, e08681.
750 <https://doi.org/10.1016/j.heliyon.2021.e08681>

751 Lysiak, N. 2009. Investigating the migration and foraging ecology of North Atlantic right whales with
752 stable isotope geochemistry of baleen and zooplankton. Ph.D. dissertation, Boston University,
753 Boston, MA, USA.

754 Lysiak, N.S.J., Ferguson, S.H., Hornby, C.A., Heide-Jørgensen, M.P., Matthews, C.J.D., 2023. Prolonged
755 baleen hormone cycles suggest atypical reproductive endocrinology of female bowhead whales. *R*
756 *Soc Open Sci* 10. <https://doi.org/10.1098/rsos.230365>

757 Lysiak, N.S.J., Trumble, S.J., Knowlton, A.R., Moore, M.J., 2018. Characterizing the duration and severity
758 of fishing gear entanglement on a North Atlantic Right Whale (*Eubalaena glacialis*) using stable
759 isotopes, steroid and thyroid hormones in Baleen. *Front Mar Sci* 5.
760 <https://doi.org/10.3389/FMARS.2018.00168>

761 Matthews, C.J.D., Ferguson, S.H., 2015. Seasonal foraging behaviour of eastern Canada-West Greenland
762 bowhead whales: An assessment of isotopic cycles along baleen. *Mar Ecol Prog Ser* 522, 269–286.
763 <https://doi.org/10.3354/meps11145>

764 McAninch, E.A., Bianco, A.C., 2014. Thyroid hormone signaling in energy homeostasis and energy
765 metabolism. *Ann N Y Acad Sci* 1311, 77–87. <https://doi.org/10.1111/nyas.12374>

766 McEwen, B.S., Wingfield, J.C., 2010. What is in a name? Integrating homeostasis, allostasis and stress.
767 Horm Behav 57, 105–111. <https://doi.org/10.1016/j.yhbeh.2009.09.011>

768 Mullur, R., Liu, Y.-Y., Brent, G.A., 2014. Thyroid Hormone Regulation of Metabolism. Physiol Rev 94, 355–
769 382. <https://doi.org/10.1152/physrev.00030.2013>

770 Nelson, T.A., Duffus, D.A., Robertson, C., Feyrer, L.J., 2008a. Spatial-temporal patterns in intra-annual
771 gray whale foraging: Characterizing interactions between predators and prey in Clayquot Sound,
772 British Columbia, Canada. Mar Mamm Sci 24, 356–370. [https://doi.org/10.1111/j.1748-
773 7692.2008.00190.x](https://doi.org/10.1111/j.1748-7692.2008.00190.x)

774 Newell, C.L., Cowles, T.J., 2006. Unusual gray whale *Eschrichtius robustus* feeding in the summer of 2005
775 off the central Oregon Coast. Geophys Res Lett 33, L22S11. <https://doi.org/10.1029/2006GL027189>

776 Nicoloff, J.T., Fisher, D.A., Appleman, M.D., 1970. The role of glucocorticoids in the regulation of thyroid
777 function in man. Journal of Clinical Investigation 49, 1922–1929.
778 <https://doi.org/10.1172/JCI106411>

779 Pallin, L.J., Kellar, N.M., Steel, D., Botero-Acosta, N., Baker, C.S., Conroy, J.A., Costa, D.P., Johnson, C.M.,
780 Johnston, D.W., Nichols, R.C., Nowacek, D.P., Read, A.J., Savenko, O., Schofield, O.M.,
781 Stammerjohn, S.E., Steinberg, D.K., Friedlaender, A.S., 2023. A surplus no more? Variation in krill
782 availability impacts reproductive rates of Antarctic baleen whales. Glob Chang Biol 29, 2108–2121.
783 <https://doi.org/10.1111/gcb.16559>

784 Peterson, B.J., Fry, B., 1987. Stable isotopes in ecosystem studies. Annu Rev Ecol Syst 18, 293–320.
785 <https://doi.org/10.1146/annurev.es.18.110187.001453>

786 Pirotta, E., Thomas, L., Costa, D.P., Hall, A.J., Harris, C.M., Harwood, J., Kraus, S.D., Miller, P.J.O., Moore,
787 M.J., Photopoulou, T., Rolland, R.M., Schwacke, L., Simmons, S.E., Southall, B.L., Tyack, P.L., 2022.
788 Understanding the combined effects of multiple stressors: A new perspective on a longstanding
789 challenge. Science of The Total Environment 821, 153322.
790 <https://doi.org/10.1016/j.scitotenv.2022.153322>

791 Reckendorf, A., S.U., P.E., & D.K., 2023. Marine Mammals. Springer International Publishing, Cham.
792 <https://doi.org/10.1007/978-3-031-06836-2>

793 Rice, D.W., Wolman, A.A., 1971. Life history and ecology of the gray whale (*Eschrichtius robustus*),
794 American Society of Mammalogists. American Society of Mammalogists, Stillwater, Oklahoma.

795 Riekenberg, P.M., Camalich, J., Svensson, E., IJsseldijk, L.L., Brasseur, S.M.J.M., Witbaard, R., Leopold,
796 M.F., Rebolledo, E.B., Middelburg, J.J., van der Meer, M.T.J., Sinninghe Damsté, J.S., Schouten, S.,
797 2021. Reconstructing the diet, trophic level and migration pattern of mysticete whales based on
798 baleen isotopic composition. *R Soc Open Sci* 8. <https://doi.org/10.1098/rsos.210949>

799 Rolland, R.M., Parks, S.E., Hunt, K.E., Castellote, M., Corkeron, P.J., Nowacek, D.P., Wasser, S.K., Kraus,
800 S.D., 2012. Evidence that ship noise increases stress in right whales. *Proceedings of the Royal*
801 *Society B: Biological Sciences* 279, 2363–2368. <https://doi.org/10.1098/rspb.2011.2429>

802 Romero, L.M., Dickens, M.J., Cyr, N.E., 2009. The Reactive Scope Model - a new model integrating
803 homeostasis, allostasis, and stress. *Horm Behav* 55, 375–89.
804 <https://doi.org/10.1016/j.yhbeh.2008.12.009>

805 Romero, M.L., Wingfield, J.C., 2016. *Tempests, poxes, predators, and people: stress in wild animals and*
806 *how they cope* Oxford University Press (Oxford, UK).

807 Saupe, S.M., Schell, D.M., Griffiths, W.B., 1989. Carbon-isotope ratio gradients in western arctic
808 zooplankton. *Mar Biol* 103, 427–432. <https://doi.org/10.1007/BF00399574>

809 Schell, D.M., Saupe, S.M., Haubenstock, N., 1989. Bowhead whale (*Balaena mysticetus*) growth and
810 feeding as estimated by $d^{13}C$ techniques. *Mar Biol* 103, 433–443.
811 <https://doi.org/10.1007/BF00399575>

812 Stewart, J.D., Joyce, T.W., Durban, J.W., Calambokidis, J., Fauquier, D., Fearnbach, H., Grebmeier, J.M.,
813 Lynn, M., Manizza, M., Perryman, W.L., Tinker, M.T., Weller, D.W., 2023. Boom-bust cycles in gray
814 whales associated with dynamic and changing Arctic conditions. *Science* (1979) 382, 207–211.
815 <https://doi.org/10.1126/science.adi1847>

816 Stewart, J.D., Weller, D.W., 2021. Abundance of Eastern North Pacific gray whales 2019/2020. NOAA
817 Technical Memorandum NMFS-SWFSC-639.

818 Sumich, J.L., 2001. Growth of baleen of a rehabilitating gray whale calf. *Aquat Mamm* 27.3.

819 Suryan, R.M., Arimitsu, M.L., Coletti, H.A., Hopcroft, R.R., Lindeberg, M.R., Barbeaux, S.J., Batten, S.D.,
820 Burt, W.J., Bishop, M.A., Bodkin, J.L., Brenner, R., Campbell, R.W., Cushing, D.A., Danielson, S.L.,
821 Dorn, M.W., Drummond, B., Esler, D., Gelatt, T., Hanselman, D.H., Hatch, S.A., Haught, S.,
822 Holderied, K., Iken, K., Irons, D.B., Kettle, A.B., Kimmel, D.G., Konar, B., Kuletz, K.J., Laurel, B.J.,
823 Maniscalco, J.M., Matkin, C., McKinstry, C.A.E., Monson, D.H., Moran, J.R., Olsen, D., Palsson, W.A.,

824 Pegau, W.S., Piatt, J.F., Rogers, L.A., Rojek, N.A., Schaefer, A., Spies, I.B., Straley, J.M., Strom, S.L.,
825 Sweeney, K.L., Szymkowiak, M., Weitzman, B.P., Yasumiishi, E.M., Zador, S.G., 2021. Ecosystem
826 response persists after a prolonged marine heatwave. *Sci Rep* 11, 6235.
827 <https://doi.org/10.1038/s41598-021-83818-5>

828 Swartz, S.L., Taylor, B.L., Rugh, D.J., 2006. Gray whale *Eschrichtius robustus* population and stock
829 identity. *Mamm Rev*. <https://doi.org/10.1111/j.1365-2907.2006.00082.x>

830 Teixeira, C.R., Troina, G.C., Daura-Jorge, F.G., Simões-Lopes, P.C., Botta, S., 2022. A practical guide on
831 stable isotope analysis for cetacean research. *Mar Mamm Sci*. <https://doi.org/10.1111/mms.12911>

832 Thomas, P.O., Reeves, R.R., Brownell, R.L., 2016. Status of the world's baleen whales. *Mar Mamm Sci* 32,
833 682–734. <https://doi.org/10.1111/mms.12281>

834 Torres, L.G., Bird, C.N., Rodríguez-González, F., Christiansen, F., Bejder, L., Lemos, L., Urban R, J., Swartz,
835 S., Willoughby, A., Hewitt, J., Bierlich, K.C., 2022. Range-wide comparison of gray whale body
836 condition reveals contrasting sub-population health characteristics and vulnerability to
837 environmental change. *Front Mar Sci* 9. <https://doi.org/10.3389/fmars.2022.867258>

838 Torres, L.G., Brander, S.M., Parker, J.I., Bloom, E.M., Norman, R., Van Brocklin, J.E., Lasdin, K.S.,
839 Hildebrand, L., 2023. Zoop to poop: assessment of microparticle loads in gray whale zooplankton
840 prey and fecal matter reveal high daily consumption rates. *Front Mar Sci* 10.
841 <https://doi.org/10.3389/fmars.2023.1201078>

842 Trueman, C.N., St John Glew, K., 2019. Isotopic tracking of marine animal movement, in: *Tracking animal*
843 *migration with stable isotopes*. <https://doi.org/10.1016/B978-0-12-814723-8.00006-4>

844 Wasser, S.K., Lundin, J.I., Ayres, K., Seely, E., Giles, D., Balcomb, K., Hempelmann, J., Parsons, K., Booth,
845 R., 2017. Population growth is limited by nutritional impacts on pregnancy success in endangered
846 Southern Resident killer whales (*Orcinus orca*). *PLoS One* 12, e0179824.
847 <https://doi.org/10.1371/journal.pone.0179824>

848 Williams, C.T., Chmura, H.E., Zhang, V., Dillon, D., Wilsterman, K., Barnes, B.M., Buck, C.L., 2019.
849 Environmental heterogeneity affects seasonal variation in thyroid hormone physiology of free-
850 living arctic ground squirrels (*Urocitellus parryii*). *Can J Zool* 97, 783–790.
851 <https://doi.org/10.1139/cjz-2018-0302>

852 Wilsterman, K., Buck, C.L., Barnes, B.M., Williams, C.T., 2015. Energy regulation in context: Free-living
853 female arctic ground squirrels modulate the relationship between thyroid hormones and activity
854 among life history stages. *Horm Behav* 75. <https://doi.org/10.1016/j.yhbeh.2015.09.003>

855 Wingfield, J.C., 2005. The concept of allostasis: coping with a capricious environment. *J Mammal* 86,
856 248–254. <https://doi.org/10.1644/BHE-004.1>

857 Wingfield, J.C., Maney, D.L., Breuner, C.W., Jacobs, J.D., Lynn, S., Ramenofsky, M., Richardson, R.D.,
858 1998. Ecological bases of hormone—behavior interactions: The “Emergency life history stage.” *Am*
859 *Zool* 38, 191–206. <https://doi.org/10.1093/icb/38.1.191>

860